

2021-03-12

WORST CASE OVERHEAD TRANSMISSION LINE PARAMETER ANALYSIS IN THE PRESENCE OF UNCERTAINTY USING MONTE CARLO AND INTERVAL ARITHMETIC APPROACH

MOGESIE, SHIFERAW TESSEMA

<http://ir.bdu.edu.et/handle/123456789/12444>

Downloaded from DSpace Repository, DSpace Institution's institutional repository



BAHIR DAR UNIVERSITY
BAHIR DAR INSTITUTE OF TECHNOLOGY
SCHOOL OF RESEARCH AND POSTGRADUATE STUDIES
FACULTY OF ELECTRICAL AND COMPUTER ENGINEERING

**WORST CASE OVERHEAD TRANSMISSION LINE
PARAMETER ANALYSIS IN THE PRESENCE OF UNCERTAINTY
USING MONTE CARLO AND INTERVAL ARITHMETIC
APPROACH**

BY

MOGESIE SHIFERAW TESSEMA

ADVISOR: YOSEPH MEKONEN (Dr.)

Bahir Dar, Ethiopia

March 12, 2021



BAHIR DAR UNIVERSITY
BAHIR DAR INSTITUTE OF TECHNOLOGY
SCHOOL OF POST GRADUATE STUDIES
FACULTY OF ELECTRICAL AND COMPUTER ENGINEERING

**WORST CASE OVERHEAD TRANSMISSION LINE PARAMETER
ANALYSIS IN THE PRESENCE OF UNCERTAINTY USING MONTE
CARLO AND INTERVAL ARITHMETIC APPROACH**

A Thesis Submitted to the School of Research and Graduate Studies of Bahir Dar
Institute of Technology, Bahir Dar University

In Partial Fulfillment of the Requirements for the Degree of MASTERS in the Power
Systems Engineering in the Faculty of Electrical and Computer Engineering.

MOGESIE SHIFERWA TESSEMA

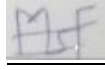
ADVISOR: YOSEPH MEKONEN (Dr.)

Bahir Dar, Ethiopia

DECLARATION

I declare that this MSc thesis is my original work, has not been presented for the fulfillment of an MSc degree in this or any other university, and all sources and materials used for the thesis have been acknowledged.

Name of the student: Mogesie Shiferaw Tessema

Signature: 

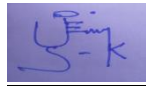
Date of submission: 02/02/2021

Place: Bahir Dar, Ethiopia

This thesis has been submitted for examination with my approval as a university advisor.

Advisor Name: Dr. Yoseph Mekonen

Advisor's Signature:



© February 02, 2021

MOGESIE SHIFERAW TESSEMA

WORST CASE OVERHEAD TRANSMISSION LINE PARAMETER
ANALYSIS IN THE PRESENCE OF UNCERTAINTY USING MONTE
CARLO AND INTERVAL ARITHMETIC APPROACH

ALL RIGHTS RESERVED

BAHIR DAR UNIVERSITY
BAHIR DAR INSTITUTE OF TECHNOLOGY
SCHOOL OF RESEARCH AND GRADUATE STUDIES
FACULTY OF ELECTRICAL AND COMPUTER ENGINEERING
THESIS APPROVAL SHEET

Student Name : Mogesie Shiferaw Tessema Signature: [Signature] Date: 11/03/2021

The following graduate faculty members certify that this student has successfully presented the necessary written final thesis and oral presentation for partial fulfillment of the thesis requirements for the Degree of Master of Science in Power Systems Engineering.

Approved by Board of Examiners

Yoseph Mekonen (Dr.)
Advisor's name

[Signature]

02/02/2021

Signature

Date

Getachew Biru (Dr.-Ing)
External Examiner's name

[Signature]

11/03/2021

Signature

Date

Tassew Tadiwose (Dr.)
Internal Examiner's name

[Signature]

11/03/2021

Signature

Date

Mr. Abirham Hizkiel
Chair man's name

[Signature]

11/03/2021

Signature

Date

Mr. Biniyam Zemene
Program Chair Holder's name

[Signature]

11/03/2021

Signature

Date

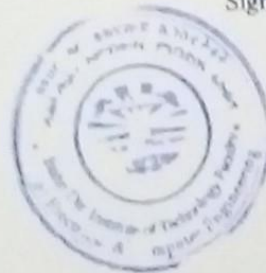
Mr. Tewodros Gera
Faculty Dean's name

[Signature]

11/03/2021

Signature

Date



Acknowledgment

First of all, I would like to thank the Almighty God for his provision of Grace to complete the entire work. Secondly, I would like to thank my mother for her heart full support during all challenges and for praying to GOD for me. And also, I would like to express my thanks to express my deepest gratitude to my advisor, Yoseph Mekonen (Dr.) for his patience, guidance, encouragement, and support in shaping the outlook of this thesis. He provided invaluable insights that have guided my thinking and understanding. Finally to those who encouraged me and showed me great affection throughout this thesis work, my sincere thank is here, Thank you all!!!

Mogesie Shiferaw Tessema

Abstract

Above 98% of the Ethiopian electric power transmission types are Over Head transmission line (OHTL) which are an outdoor system. In addition to load variation and Generation change, OHTL sag, tension, and conductor length variation due to weather fluctuation are also other problems for reliable power delivery. Without reliable power delivery, power generation is just simply a waste of resources. Mostly Ethiopian Electric power system delivery is interrupted because of OHTL failure by different factors. It can be easily affected by weather changes such as variation of temperature due to thermal expansion and elastic elongation. Additionally, the horizontal wind pressure and vertical ice loading make the value of sag, tension, and conductor length vary in a range of values. Such changes make the calculated data uncertain and require analysis of OHTL parameters with uncertainty. The temperature and conductor length variation affects the resistance of OHTL. This variation leads to voltage drop and power loss, which is mostly considered as load variation and other disturbances. To calculate resultant weight, sag, tension, cable length, and resistance of an OHTL, Interval Arithmetic (IA) and Monte Carlo (MC) approaches based on uncertainty concept for a catenary curve is proposed. The results based on the two methods are compared and analyzed with 400kV OHTL from Bahir Dar to Addis Abeba of the case study area. From 10 cities the worst affected is Addis Ababa city with the uncertain results of resultant weight varies from the minimum 21.1912 kg/m to 27.7765 kg/m, the tension changes from 10685.87 N to 9893.24 N, the sag and conductor length changes from the minimum 2.7935 m and 123.5112 m to 6.0759 m and 124.1431 m, respectively. Also, the least affected is Bura city varies from the minimum 21.0814 kg/m to 21.4765 kg/m, the tension changes from 9950.6208 N to 9671.7312 N, the sag and conductor length changes from the minimum 3.5195 m and 123.6103 m to 3.6772 m, and 123.6348 m, respectively. The IA based result gives a more conservative bound than the MC method in all the cases.

Keywords: IA; MC; Sag; Tension; Transmission line

Table of contents

Acknowledgment.....	i
Abstract.....	ii
Table of contents	iii
List of tables.....	vi
List of figures	viii
Acronym and abbreviations	ix
Chapter 1.....	1
Introduction.....	1
1.1 Background.....	1
1.2 Statement of the problem.....	4
1.3 Objectives of the Thesis	5
1.4 Significance of the study	5
1.5 Scope and Limitations	6
1.6 Methodology.....	6
1.7 Organization of the thesis	6
Chapter 2.....	8
Literature Review	8
Chapter 3.....	21
Mathematical modeling and analysis	21
3.1. Theory of overhead transmission line	21
3.1.1 Introduction.....	21
3.1.2 Main elements of OHTL.....	22
3.1.3 The OHTL parameters	23
3.2 The effect of ice loading and wind pressure in OHTL	24
3.3 Catenary model of OHTL.....	26
3.4 Temperature change in OHTL	32
3.4.1 Thermal Elongation	32

3.4.2 Stress-Strain Behavior	33
3.5 Interval Arithmetic approach	37
3.6 Monte Carlo approach	38
3.7 Case Study area of the thesis.....	40
Chapter 4.....	41
Results and conclusion	41
4.1 Results	41
4.1.1 OHTL parameters of Bahir Dar city	41
4.1.2 OHTL parameters of Dangila city	43
4.1.3 OHTL parameters of Enjibara city	45
4.1.4 OHTL parameters of Bura city.....	47
4.1.5 OHTL parameters of Finote Selam.....	49
4.1.6 OHTL parameters of Debre Markos city	51
4.1.7 OHTL parameters of Dejen city	53
4.1.8 OHTL parameters of Gerbe Gurach city.....	55
4.1.9 OHTL parameters of Ficha city.....	57
4.1.10 OHTL parameters of Addis Ababa city	59
4.2 Discussion.....	61
Chapter 5.....	66
Conclusion and recommendations.....	66
5.1 Conclusion	66
5.2 Recommendation.....	66
Reference	68
Appendix.....	76
Appendix A. Metrological data of 10 cities	76
Appendix A. 1. Temperature annual data in degree centigrade	76
Appendix A. 2. Wind speed annual data in m/s.....	77
Appendix B. Sag and tension data of case study area.....	79
Appendix C. Mat lab codes to generate results.....	80
Appendix C. 1. Mat lab codes for IA	80

Appendix C. 2. Mat lab codes for MC	81
Appendix D. Contents of the table used for result demonstration	83
Appendix D. 1. Table I.....	83
Appendix D. 2. Table II.....	83
Appendix D. 3. Table III	83

List of tables

Table 4.1. Initial inputs and resistance of Bahir Dar	41
Table 4.2. Sag and conductor length of Bahirdar	41
Table 4.3. Resultant weight, tension, and resistance of Bahirdar	42
Table 4.4. Initial inputs and resistance of Dangila	43
Table 4.5. Sag and conductor length of Dangila	44
Table 4.6. Resultant weight, tension, and resistance of Dangila.....	44
Table 4.7. Initial inputs and resistance of Enjibara	45
Table 4.8. Sag and conductor length of Enjibara	46
Table 4.9. Resultant weight, tension, and resistance of Enjibara.....	46
Table 4.10. Initial inputs and resistance of Bura.....	47
Table 4.11. Sag and conductor length of Bura.....	48
Table 4.12. Resultant weight and tension of Bura	48
Table 4.13. Initial inputs and resistance of Finot Selam.....	49
Table 4.14. Sag and conductor length of Finote Selam.....	50
Table 4.15. Resultant weight, tension, and resistance of Finote Selam	50
Table 4.16. Initial inputs and resistance of Debre Markos	51
Table 4.17. Sag and conductor length of Debre Markos	52
Table 4.18. Resultant weight, tension, and resistance of Debre Markos.....	52
Table 4.19. Initial inputs and resistance of Dejen	53
Table 4.20. Sag and conductor length of Dejen	54
Table 4.21. Resultant weight, tension, and resistance of Dejen.....	54
Table 4.22. Initial inputs and resistance of Gerbe Guaracha	55
Table 4.23. Sag and conductor length of Gerbe Gurach.....	56
Table 4.24. Resultant weight, tension, and resistance of Gerbe Gurach	56
Table 4.25. Initial inputs and resistance of Ficha.....	57
Table 4.26. Sag and conductor length of Ficha.....	58
Table 4.27. OHTL resultant weight, tension, and resistance of Ficha	58
Table 4.28. Initial inputs and resistance of Addis Ababa	59

Table 4.29. Sag and conductor length of Addis Ababa	60
Table 4.30. Resultant weight, tension, and resistance of Addis Ababa.....	60

List of figures

Figure 3.1. Overhead power transmission line (OHTL).....	22
Figure 3.2. Underground power transmission line (UGTL)	22
Figure 3.3. The block diagram of the factors affecting OHTL.....	23
Figure 3.4. The effect of ice loading and wind force on OHTL	24
Figure 3.5. The ice, wind, and bare conductor loading on the cable and its resultant weight	25
Figure 3.6. Catenary shaped conductor suspended between two supports (towers)	27
Figure 3.7. Triangle formed by the tangential and horizontal component	28
Figure 3.8. Stress-Strain relationship	33
Figure 4.1. OHTL parameters variation for Bahirdar city	43
Figure 4.2. OHTL parameters variation for Dangila city	45
Figure 4.3. OHTL parameters variation for Enjibara city	47
Figure 4.4. OHTL parameters variation for Bura city.....	49
Figure 4.5. OHTL parameters variation for Finote Selam.....	51
Figure 4.6. OHTL parameters variation for Debre Markos.....	53
Figure 4.7. OHTL parameters variation for Dejen.....	55
Figure 4.8. OHTL parameters variation for Gerbe Gurach	57
Figure 4.9. OHTL parameters variation for Ficha	59
Figure 4.10. OHTL parameters variation for Addis Ababa	61

Acronym and abbreviations

AA	Affine arithmetic
AAAC	All aluminum alloy conductor
AC	Alternating current
ACSR	Aluminum conductor steel reinforced
CA	Classical arithmetic
DC	Direct current
DOF	Degree of freedom
EEPU	Ethiopian electric power utility
ETAP	Electrical transient analyzer program
ft	Feet
IA	Interval arithmetic
IEEE	Institute of Electrical and Electronics Engineers
kV	Kilovolt
Km	Kilometer
lb	Pound
m	Meter
m Ω	million ohms
MHz	Megahertz
MATLAB	Matrix laboratory
MC	Monte Carlo
Mpsi	Mega pound per square inch
NASA	National aeronautics and space administration
NPCC	Northeast power coordinating council
NWP	Numerical weather prediction
OHTL	Overhead transmission line
PDF	Probability distribution function
PLS-CADD	Power Line Systems - Computer-Aided Design and Drafting

PMF	Probability mass function
PMU	Phasor measurement unit
su	Square Units
TLTE	Transmission line temperature evolution
UGTL	Underground transmission line

Chapter 1

Introduction

1.1 Background

The power Transmission line is an important concept in power system engineering for transmitting power from generation to distribution system. To transmit electric power from one place to the other there are two types of transmission systems, overhead, and underground transmission systems. Overhead transmission lines (OHTL) are one type of power system network, which are used to transfer electric power above the ground from the generation station to the substation and then to distribute it to the customer side [1- 3].

OHTL conductors do not directly connect between their supporting towers in a straight line, rather the shape of the conductor formed between the towers is either a catenary or a parabola. OHTL conductor mostly takes the shape of a catenary between support points because of its flexible nature and uniform weight along its length [2],[3].

In practical use, the OHTL conductors are regularly planned by the use of a catenary, while distribution lines are mostly designed by applying the parabolic shape. The catenary and parabola functions of overhead lines of electricity are significantly different from each other. The catenary is the hyperbolic function used where OHTL are above 400 Km while the parabolic is the quadratic function used where OHTL are less than 400Km [4],[5].

In OHTL the conductor is suspended between two successive towers and its weight with other factors cause the conductor to be stressed and will result in sagging. The sagging effect of the OHTL depends on the weight per unit length, horizontal tension, the elevation of the installation point, and the weather fluctuation. OHTL are highly loaded transmission lines in the summer that can sag much more than the same line in winter and tension is opposite to the sagging property [6].

OHTL conductors are affected by environmental factors like changes in temperature, wind, and ice loading. The effect of temperature changes the value of resistance and the resistance affects the current carrying capacity of the conductor [7].

Wind loading also affects the OHTL results of the conductor swinging out of synchronization. In recent years, many 220kV-500kV overhead transmission line flashovers have been caused by conductor swinging out of synchronisms [8].

The capability of an OHTL depends on its strength against wind loading, ice loading, and temperature variation. The higher the wind pressure and the ice weight on the cable, the greater chance that the cable will break and transmission is disturbed. When the temperature increases, it has an effect not only on the cable breakage but also on the current transmitted through the cable. The effect of the wind pressure and ice accumulation can result from the increasing weight of the cable to a series of accidents like breakage of the line, falling off the tower or pole, creation of fire on the forest, etc. The probability that the OHTL can cause a fire should be known to save power system equipment (pole, tower, insulators, etc.), life, and property [9],[10].

The changes that happened on the conductor because of environmental factors make the calculated data of sag, tension, conductor length, and resultant weight become uncertain and needs to consider the uncertainty principle. The theory of uncertainty is deduced from the three fundamental principles; uncertain measurement, uncertain variable, and uncertain distributions. Uncertainty is anything that can be defined by uncertain measures and which fulfills the axioms of uncertainty theory. The concept of uncertainty is based on two fundamental approaches which are probabilistic and unknown but bounded data inputs [9], [11], [13].

Analysis of OHTL parameters by considering uncertainty is also important to decrease power interruptions and to make the line reliable. The initial design has to consider the load capability of the line including environmental factors. Those factors and measuring devices' value are not absolute rather they vary between low and high extreme seasonally

and changes from place to place. The OHTL parameters are also affected by the measurement errors and the failure of data storing instruments [13],[14].

Electric utilities are now facing many uncertainties in the current economic environment. The current issue facing utilities include the fundamental need for additional generating capacity, new transmission systems, and more efficient use of existing resources. As a result, there are now many uncertainties associated with utility decisions. It is no longer valid to assume that the input parameters are known with certainty. Utilities need to understand the potential effect of variation in these parameters on the outcome of their studies and considering uncertainty based on two approaches. The first is a “probabilistic” approach where probability distributions for all of the uncertainties are assumed. The second approach is called “unknown but bounded” in which upper and lower limits on the uncertainties are assumed without probability distributions [16-18]. In this paper, the uncertainty concept is considered based on an unknown but bounded and probabilistic approach using IA and MC numerical analysis methods respectively.

Ramon Moore introduced Interval Arithmetic (IA) in the 1960s as an approach to bound rounding errors in mathematical computation. The theory of IA emerged considering the computation of both the exact solution and the error term as a single entity and it is a very powerful technique with numerous applications in engineering. In the same way classical arithmetic (CA) operates on real numbers, one of the original motivations for the creation of interval arithmetic was automatic and round-off error analysis by defining a set of operations on intervals. There are usually three sources of error while performing numerical computations: rounding, truncation, and input errors. IA considers uncertainty based on unknown but bounded and it acknowledges the limitation of using a single floating-point number approximation method [15],[16].

Similarly, the Monte Carlo (MC) method is a class of numerical approach based on generating random sampling. It takes a small, randomly-drawn sample from a given test data and estimating the desired output from the given sample. It also considers uncertainty based on the probabilistic approach [17], [18].

Because of the variation of weather fluctuation of ice loading, wind loading, and temperature change, the overall OHTL parameters cannot be calculated with certainty [13].

Therefore, for calculating OHTL loading, sag, tension, cable length, and worst-case resistance value, by considering the uncertainty concept, IA, MC methods are formulated. The conducted methods are tested by using case studies of 400kV OHTL emanating from Bahir Dar and reaches to Addis Ababa.

1.2 Statement of the problem

In an electrical power system, a generated power from the generating station to a customer side is transmitted through an overhead transmission line. In the worst-case scenario, OHTL failure leads to huge damage to humans and resources resulting in power interruption and unbalance of the system. In rural areas, it may lead to creation fire on forests, which is so expensive to mitigate. The factors that lead to OHTL failure are variation in the transmission line sag, tension, and conductor length caused by temperature and wind loading. When temperature change results in thermal expansion and elongation on the conductor, horizontal wind pressure and vertical ice accumulation create loading on the conductor. The temperature and cable length variations have also an effect on the resistance of the OHTL. This variation leads to a variable voltage drop, which is mostly considered with load variation, and then load variation leads to power interruption. Such changes make the calculated data uncertain and require an uncertainty concept.

To calculate the resultant loading value of sag and tension of OHTL, an uncertainty concept based on IA and MC methods is required. The two methods are applied to provide the worst case result in OHTL to protect the transmission system from unexpected changes once the line is installed.

These days, it is the fact that when heavy rain and wind pressure is coming to the Ethiopian electric system, operators mostly in the distribution system, make the power

line to be switch off, because of the weather effect, and hence the customers will be disturbed.

This thesis focuses on the problems of OHTL parameter change due to weather fluctuation on the 400kV Ethiopian transmission line from Bahir Dar to Addis Ababa city and investigating the techniques to quantify and the uncertainties for reliable power delivery.

1.3 Objectives of the Thesis

General objective

The general objective of this thesis is to study the worst effect of weather change on OHTL using boundary and probabilistic based approaches on the Ethiopian 400kV transmission line.

Specific objectives

The specific objectives of this research are as follows:

- ❖ To collect and analyze the data of weather conditions and the parameters of 400kV OHTL from Bahir Dar to Addis Ababa.
- ❖ To carry out the basic mathematical analysis of the OHTL.
- ❖ To incorporate the weather uncertainties in the basic OHTL model.
- ❖ To formulate mathematically the IA and MC approach for the OHTL.
- ❖ To formulate a Mat lab code for the two methods using the formulated equations.
- ❖ To make a comparative study among the two methods and present the result.
- ❖ To draw relevant conclusions and make recommendations for analysis of OHTL parameters while considering uncertainty.

1.4 Significance of the study

- ❖ It will be a good reference for future researchers related to OHTL parameters while considering uncertainty.
- ❖ It will be important for EEPU while installing the new OHTL.

- ❖ It will Maintain the life span of OHTL equipment's, like a pole, tower, conductor, cross arm, insulator, etc.,
- ❖ Decrease power interruption and deliver reliable power to the customer side.
- ❖ Save humans and animal life from shocking by different cases during weather change.
- ❖ Eventually, it will provide the worst-case result for the installation of a new transmission line in that area.

1.5 Scope and Limitations

This research is conducted on a case study of a specific area and conducted by Math lab software. Uncertainties in the temperature and the wind have been included in analyzing the OHTL parameters. The effect of the uncertainties are quantified and presented using MC and IA approaches. Due to the presence of our country in the tropical climate zone, our country's transmission lines are not affected by ice loading. As a result, the effect of ice on the calculation of the OHTL parameters is not included.

1.6 Methodology

The research is conducted by following some steps as follows:

The first method is reviewing different related papers to this thesis. The materials can be published or unpublished such as Journal papers, conference papers, articles, books, etc. The second method is the data are collected from different institutions like Northwest Ethiopian electric power utility Bahir Dar district and NASA. Next to this, the collected data are analyzed. The third method is also, formulation of OHTL parameters by using IA and MC with the presence of uncertainty. The next is the analysis of the case study area by comparing the methods and also result in a demonstration is done. Lastly, depending on the analysis the conclusion is made and a recommendation is given.

1.7 Organization of the thesis

This thesis is organized into five chapters as follows: Chapter one gives a general introduction to this study with emphasis on the effect of weather conditions on OHTL parameters, relevance, and objective of the study. Chapter two more discusses the

literature review of different studies, which are related to this research. Chapter three deals with the data analysis, mathematical modeling, and also some description about the case study area. Chapter four deals with the discussion and the result of the study. Chapter five ends with the conclusion and recommendation of this study.

Chapter 2

Literature Review

In this chapter, the basics of overhead transmission lines and the effect of temperature variation, wind loading, and ice accumulation on it will be presented according to the research work which has been done in the area.

Keshavarzian, Mehran; Priebe, Charles H., presented sag and tension calculation of transmission line at different temperature values using the ruling span concept based on the rotational stiffness of suspension insulator strings. To decrease unacceptable errors by using the ruling span concept while calculating the value of sag and tension with unequal spans, they have used multi-span line segments at different temperatures. A simple equation, based on the parabolic approximation, is derived to calculate changes in the span lengths, conductor sags, and tensions. The method follows the ruling span concept but relaxes the fundamental assumptions of the ruling span method. The accuracy of the method is compared with the more complex, nonlinear, finite element method. A general procedure for the evaluation of conductor sags and tensions of a level transmission line which includes the force balance at each suspension clamp has been presented. Lastly, they have developed the procedure depending on the traditional ruling span concept [19]. In this paper, the modern method to calculate sag and tension is used, and derivation of the equation to calculate sag and tension and the derivation of the formulas for sag and tension depending on a catenary curve are not studied.

Adomah, K.; Mizuno, Y.; Naito, K. have been discussed the assessment of the reduction in tensile strength of an overhead transmission line's conductor by climatic change. The methods they have used to analyze the problem are one of the uncertainty based technique. They have also assessed the tensile strength of overhead transmission lines in response to growing load and different failures related to climatic change. They have concluded that the main factors to determine a conductor's life are growing load and

climatic change. This paper also recommended that this analysis is a very useful guide to planning engineers [20].

In this paper, the uncertainty analyzing method ‘unknown but bounded’ and the impact of climatic change on overhead transmission line parameters like sag, tension, and conductor length is not studied.

Hickey, T.; Ju, Q.; Van Emden, M.H. have investigated the concept and nature of the IA numerical analysis approach. They have presented instead of using a single floating-point number as an approximation for the value of a real variable in the mathematical model under investigation, interval arithmetic acknowledges limited precision by associating with the variable. In this paper, IA operations (addition, subtraction, multiplication, and division) are defined mathematically and they provided algorithms for computing these operations assuming exact real arithmetic. And also in this paper, it has been demonstrated that one can formulate a theory of Interval Arithmetic based on extended notions of intervals which allow intervals to be unbounded and non-closed [16].

Olsen, R. G.; Edwards, K. S. have investigated the real-time monitoring of high voltage transmission line conductor sag. This paper has been done by measuring the amount of conductor sag and simple calculation. Since increasing the current causes the conductor temperature to increase, the conductor to elongate and increasing of the sag. The method involves attaching two ends of a grounded wire of high electrical resistance to an appropriate location on each of two transmission line towers and measuring the current induced on the wire by the nearby transmission line conductors. They concluded, a simple and accurate method that uses the current induced in a resistive wire to measure conductor sag has been used and changes in conductor sag of 1% have been shown to produce nearly a 10:1 change in the induced current [21]. In this paper, the effect of high voltage overhead transmission line parameters like tension, conductor length, and resistance is not considered. Also, the effect of weather conditions on the value of conductor sag is not analyzed.

Piccolo, A.; Vaccaro, A.; Villacis, D. have presented an AA based methodology for the thermal rating assessment of overhead lines in the presence of uncertainty. In this paper, the AA model is proposed for the numerical computation of overhead lines and to address the problems of thermal rating assessment. Simulation studies are presented and discussed to prove the effectiveness of the proposed methodology in addressing the problem of uncertainty analysis in both static and dynamic thermal rating assessments. They have concluded that the numerical result of the AA approach indicates an accurate solution compared to other methods [5]. However, the effect uncertainty on sag, tension, and conductor length on overhead transmission lines is not assessed and a comparison of traditional methods with modern methods was not studied.

Shaalán, Hesham has researched calculating transmission line inductance using IA. In this paper, the concept of Uncertainty has been considered i.e. uncertainty probabilistic, and the “unknown but bounded” approach is used. The author presents the IA method can be used for practical implementation and extension of the unknown but bounded concepts. Here, OHTL inductance has been calculated by both traditional and IA methods, while comparing the two methods, IA is found to be the best way and it does not need many iterations run because the total variation in the output is known given the total variation in input parameters is known [6]. In this paper, the two methods, IA and traditional single-point methods are not compared with MC numerical analysis, and the overhead transmission line parameters like sag, tension, and conductor length are not considered.

Kurokawa, Sergio; Filho, Jose Pissolato; Tavares, Maria Cristina; Portela Carlos M. and Afonso J. Prado have researched analyzing the behavior of Overhead transmission line parameters on the presence of ground wires. This paper aims to reduce the ground wire for a generic multi-phase transmission line and a specific 440kV three-phase overhead transmission line. They have reduced the ground wire by following two conditions, frequency-dependent and independent. They also presented analytical and graphical results for a 440kV three-phase overhead transmission line and real data are considered

for every frequency between 10Hz and 1MHz. The results presented in this paper were obtained with the assumption of zero transversal voltage of ground wires along the line [24]. In this paper, the effects of uncertainty and weather fluctuation on overhead transmission lines are not studied.

Abdel-Gawad, A.F.; Zoklot, A.S.A. have researched the effect of wind and environmental conditions on overhead high voltage transmission lines. In this paper, the effect of wind on high voltage transmission lines is studied experimentally by two sets of models that is a pair of tension towers and a pair of suspension towers. The two sets of models were tested using a delivery wind tunnel and three different sizes of conductors were tested at three values of the wind speed (5, 10, and 15 m/s). The author's also studied that the effect of environmental conditions and measurements of the horizontal and vertical displacement of the conductors of different phases were recorded [25].

The drawback of this paper is the mathematical modeling and the parameters of overhead transmission line conductors are not studied and simulated.

Ramachandran, Poorani; Vittal, Vijay; Heydt, Gerald Thomas presented an estimation of mechanical state for overhead transmission lines with level spans. The authors said that, because of malicious attacks and natural disasters, overhead transmission lines are in danger; this underscores the need to develop new techniques to ensure safe and reliable transmission of electric power. They have developed an online monitoring system based on mechanical state estimation to determine the sag levels of overhead transmission lines in real-time at the normal physical condition or damage. They have also used the least-squares state estimation computational algorithm which is applied to overhead transmission line equations to determine the parameters of an overhead transmission line. The authors also concluded that the estimated conductor sag levels are used to generate warning signals and displayed to the operator to make the best decisions to decrease failures [26]. In this paper, the only sag of an overhead transmission line is presented and the effect of other parameters on the change of the OHTL sag has not been presented in their work.

Muhr, M.; Pack, S.; Jaufer, S. have been researched the advantage of monitoring the overhead transmission line system. According to the paper, the overhead transmission line is used for all most all countries in the world because it is the most economical and practicable solution for energy transmission and the demand of the customers are increasing day today and the network of the transmission lines are increasing. However, to control and monitor the increased network by the oldest technique is difficult. Another factor that initiates the researcher is that mostly overhead transmission lines are faced different problems like affected by weather fluctuations, thunderstorms, damage by plants, animals, humans, etc. because of being overhead. In this paper, an overview of the existing overhead line monitoring system by thermal monitoring technique and usage and the benefit for the application are studied [27]. The drawback of this paper is, the comparison of different techniques that are used to monitor overhead transmission lines and the effect of weather conditions on an overhead transmission line is not studied.

Malhara, Sunita; Vittal, Vijay have researched the monitoring of sag and tension of a tilted transmission line using geometric transformation. In this paper, the problem that initiates the authors to conduct this research were, the severe environmental hazards, accidents, and malicious attacks leading to the failures of overhead transmission lines. They were proposed, detection of tower tilt and its effect on the sag and tension at the initial stage of the disruption as they are a very important way to ensure safe and reliable operation of the power system. To fulfill the above concept, they have used the geometric transformation method for each phase of a tilted tension section of a high voltage transmission line to evaluate line sag and tension. The method was compared with the PLS-CADD results and it is more accurate. The authors were concluded that towers tilt caused by natural events or human-made accidents on the transmission line affects the sag and tension of individual or adjoining spans [3]. In this research, the authors don't use computational algorithm methods like the traditional single point, IA, MC, and AA to include the effect of uncertainties. Moreover, the effect of conductor length and resistance of the overhead transmission line didn't been considered.

Sun, Baoqiang; Hou, Lei; Fu, Guanjun; Meng, Xiaobo; Guan, Zhicheng; Wang Liming have studied the dynamic response of overhead transmission lines to different wind speeds. In this paper, the overhead transmission line conductor swinging out of synchronization caused by wind force is a common problem on overhead transmission lines, it is also a current issue in China. In this paper, a 3 degree of freedom (DOF) dynamic model of a multi-span line suitable for analyzing wire swinging out of sync is presented. The author's studied finally finding out the relationship between the minimum interphase distance and wind speed to avoid air breakdown under different wind speeds [8]. The drawback of this paper is that except for wind loading other weather condition factors like temperature change, ice loading, etc. are not studied. Moreover, the effect of overhead transmission line parameters like sag, tension, conductor length, and resistance are not presented.

Liu, Baoding examined the need for uncertainty theory for different analyses. Liu Baoding presented the nature of uncertainty, the situation that uncertainty arises, the way which is used to analyze uncertainty, and the difference between uncertain variable and uncertain sets. In this paper, the relation and difference of uncertainty, fuzziness, and probability are discussed briefly. Additionally, the two uncertainty approaches that are probabilistic and unknown but bounded approaches are studied and presented to be effective if they are used in any engineering and physical world with uncertainties [11].

Oluwajobi, F; Ale, O; Ariyanninuola, A have researched the factors affecting sag in conductors while erecting overhead transmission lines. The authors presented that if the conductors are too much stretched between supports, the stress in the conductor may reach unsafe value and leads to the conductor breaking. If the sag of the conductor's very maximum, the clearance between the conductor and the earth is minimum and this leads to damage to animals, humans, plants, etc. To reduce this problem the tension in the conductor should be low to avoid the mechanical failure of the conductor and to permit the use of less strong supports and also the effects of sag on electrical construction were examined by the authors [2]. In this paper, the different methods that are used to analyze

sag are not presented and also the parameters of overhead transmission line like conductor length and resistance are not discussed. The effect of uncertainty is not considered here.

Islam, Saiful; Islam, Foredul have researched the impact of weather condition fluctuation like temperature variation, solar radiation, wind loading, on overhead transmission line conductor. Researchers presented that current-carrying overhead transmission line conductors are not only dependent upon different faults but also depend upon weather condition changes. In this paper, the relationship between the factors that affect overhead transmission line conductor (ACSR) is discussed briefly. The authors concluded that the overall current carrying capacity of the conductor increases with the decrease of ambient temperature [7]. In this paper, the analysis of the overhead transmission line conductor parameters, with weather condition fluctuation except for its current carrying capacity, is not presented briefly. Moreover, mathematical modeling based on the type of conductor shape is not studied.

Shaalán, Hesham; Point, Kings have investigated transmission line analysis using interval mathematics. In this paper, the main factor of electric utilities facing as a problem was found to be the presence of uncertainty. Also, interval mathematics is a tool for the practical implementation and extension of the unknown but the bounded concept of uncertainty has been studied. The calculation of sag, conductor length, and inductance value by a standard single point and interval mathematics method is performed, and also the comparison is done to illustrate the importance of interval mathematics [28].

Chen, Shao Qing; Li, Jian Ming; Luo, Tao; Zhou, Hui Ying; Ma, Qi Xiao; Du, Lin researched on overhead transmission lines to analyze the performance of overvoltage transducer. The authors proposed, a contactless overvoltage transducer for overhead transmission line overvoltage monitoring, since monitoring overvoltage is a key point for the security of the power transmission line. They have also performed the arrangement of the voltage divider to measure the voltage of the overhead transmission line, calculating

stray capacitance and analyzing the influence factor on sensors. They concluded that the performance and accuracy of the overvoltage transducer were proved by the AC voltage and lightning overvoltage test [29]. In this paper, the effect of overvoltage on an overhead transmission line parameter is not presented.

Polevoy, Alex has done his research on the impact of data errors on sag calculation accuracy for the overhead transmission lines. The author has identified the problem of sag value variation because of conductor properties, dispersion, and measurement errors. The author also presented, a total error of sag calculation is calculated as a weighted sum of partial errors of six measured parameters involved in the state equation, and the formula for weighting factors for partial error is obtained by differentiating the state equation and analysis of the contribution of each error. The author has shown that the error in sag and temperature measurements during stringing operation is large and these errors directly contribute to the final sag error, but errors in elasticity modules or creep values are small. The authors concluded that the absolute error of sag calculation for the ACSR conductor is about 1.5 m for a 350-m span and about 2 m for a 500–600 m span. The absolute sag error for the AAAC Al59 conductor is 25% less [30]. Even though this paper has done a breakthrough it presents only the effect of sag but didn't consider the effect of tension and conductor length altogether.

Sivanagaraju, Gangavarapu; Chakrabarti, Saikat; Srivastava, S. C. have researched estimation and impact on line current differential protection in transmission lines in the presence of uncertainty. The authors have presented a method to estimate the transmission line parameter using synchrophasor measurements from phasor measurement units, and also hybrid measurements from phasor measurement units and supervisory control and data acquisition systems. They have also proposed a method to estimate transmission line parameter uncertainties like the measurement errors. The authors proposed a new current differential protection scheme for transmission line protection using synchronized measurements and the effect of parameter uncertainty on the protection scheme is also has been investigated [31]. However, the effect of

uncertainties related to weather condition fluctuation is not considered except those uncertainties related to measurement errors.

Hatibovic, Alen studied the derivation of the equation for conductor and sag curves of an overhead transmission line based on a given catenary constant. The author's presented that, the catenary-based calculation is generally used for high voltage overhead line design and does not have limitations but in comparison to the parabola it is complicated. Since, overhead transmission lines are passed through different geographical areas and are affected by different factors like weather fluctuation, thunderstorms, etc. there must be such considerations. Hence, derivation of the equation for the overhead transmission line parameters using the catenary curve is a very important concept to maintain the health of the conductor. The authors also presented the way of the derivation of new equations for the conductor and sag curves based on a known catenary constant, which refers to the chosen conductor type, span length, tension, and temperature of the overhead line [32].

Abebe, Yoseph Mekonen have researched overhead transmission line sag, tension, and conductor length calculation using the AA technique. In the presence of uncertainty, AA has proposed for numerical calculation of the addressed problems and tested for different test cases. The researchers have presented how a weather change affects the OTL parameters and proposed an uncertainty based analysis to get the worst-case scenario results. [9].

Htalele, Tlotlollo; Du, Shengzhi have presented an analysis of power transmission line uncertainties. The overhead transmission lines are faced with failures by the effect of both environmental and physical uncertainties. The status and degree of occurrence of uncertainty in the power transmission line have been discussed. In this paper, the IA method is used for analyzing and stretching and the unknown but bounded variables in the uncertainty concept. They have also presented a comparison of the methods with synch phasor and MC method and IA found to be more versatile compared to others and

the unknown variable is stretched within the bounds. They have concluded as; IA method is faster than the other techniques [12]. However, overhead transmission line parameters like sag, tension, and conductor length with the presence of uncertainty are not discussed.

Abebe, Yoseph Mekonnen; Rao, P. Mallikarjuna; Naik, M. Gopich examines the analysis of overhead transmission line parameters with uncertainty. They have presented that in the worst-case scenario, weather fluctuations like temperature, wind loading, and ice accumulation is affecting the overhead transmission line parameters like sag, tension, conductor length, and resistance. They have also used uncertainty analysis based on AA and comparison of the method to IA and MC are discussed. Depending on the test result they have concluded that the AA method gives a slightly conservative bound than MC and IA [13]. The drawback of this paper is the basic equations derived by considering the span as a parabolic curve (short span) which is feasible only in short transmission and distribution lines and the test data are not real which random data.

Yao, Rui; Sun, Kai; Liu, Fen; Mei, Shengwei have presented an efficient simulation of temperature evaluation of overhead transmission lines based on analytical solution and NWP (Numerical weather prediction). This research has been conducted based on analytical solutions and NWP data in the presence of uncertainty in environmental parameters of temperature in both the planning stage and real-time operation. They have used a 14-bus NPCC (Northeast power coordinating council) system to check its efficiency and potential of the online risk assessment method. This paper proposed an efficient and approximate method for the TLTE (Transmission line temperature evolution). Finally, the analytical solutions together with NWP can be utilized as the methods for monitoring and security analysis of transmission systems [33]. The gap of this paper is that the effect of weather conditions like wind loading, and ice accumulation is not studied.

Sacerdotianu, Dumitru; Nicola, Marcel; Nicola, Claudiu, Ionel; Lazarescu, Florica have studied the continuous monitoring of sag of the overhead electricity transmission cables based on the measurement of their slope. In this paper, the increasing number of society

requires an increasing energy demand, and electricity consumption is increasing constantly. The increasing demand results in the existing transmission line will be overloaded and requires new methods of an electricity transmission line, and also sag is sensitive to different factors. To address the problem a mathematical model based on the catenary curve is proposed by the authors for the continuous monitoring of sag. The authors presented the result obtained according to the method showed that the system could meet the technical requirements for measuring conductor sag of overhead transmission lines [34]. Like most of the authors, the effect of weather conditions on the value of sag is not presented, and also measurement error is not considered in this paper even though it worth a shot.

Molaei, Amir has researched extracting the sagging profile of overhead power transmission lines by image processing. The problem that initiates the authors were the effect of sagging on the transmission line conductors which have a great influence on the safety, reliability, and efficiency of power transmission and also reducing the line sagging induces high tension in the conductor leads to the damaging of the conductor. To overcome the problem the author proposes as transmission lines must be designed to guarantee the maximum static loading capacity and maintaining the vertical clearance between the cables and the ground. The methods used in this paper were the mathematical formulations that are developed with the image processing method applied for inspection of cable sagging. The authors also used a designed reconfigurable experimental setup to investigate the validity of the proposed method to provide various sagging profiles and the sagging profile is extracted via image processing and the result is compared to that of an analytical method [6]. One of the shortcomings of this paper is that factors that affect sag are not studied briefly.

Noor, et al. have been studied the impact of temperature and wind on sag and tension of AAAC overhead transmission line. Noor presented the performance of the transmission line mostly depends on the resistance, capacitance, and inductance. To decrease the capacitance effect the transmission lines are connected in a curve which is catenary and

termed as sag. The author also presented, to make sag and tension in the safe limit a simulation set up to calculate sag and tension of AAAC overhead transmission line for multiple spans with the impact of different weather conditions like temperature and wind. The simulations were carried out by ETAP software [35]. However, quantifying the uncertainties is not well presented in the paper.

Hatibovic, Alen; Kadar, Peter presented an algorithm for the parabolic approximation of the catenary cable applicable in both level and inclined span. Mostly different literature ensures the solution of a level span only and the difference between the two curves is not briefly studied, this is one of the problems of this paper. The author's goal was to derive a universal equation for the catenary model by approximation of the parabola method which can be applied in all spans. The authors also present the mathematical background with algorithms and practical applications [4].

Jiang, Jintao; Jia, Zhidong; Wang, Xilin; Wang, Shihao; Yang Changjian have studied the analysis of overhead transmission line conductor sag change after the bare overhead conductor is covered with insulation material. Insulating material affects overhead transmission line conductors in some special areas like crossing forests and influences the value of the original conductor sag. Based on the conductor catenary equation, this paper evaluates the variation of conductor sag after insulation modification by analyzing the stress on the conductor, focusing on the influence of the material and thickness of the insulation on the conductor sag; and then the influence of the weight of the automatic coating device on the conductor during the insulation modification process has been analyzed and discussed [5]. Another uncertainty cause besides the weight of the insulator has not been studied by the authors. Moreover, the effect of insulation on the Ethiopian transmission line is not present since our transmission lines are not coated with insulators.

Asprou, Markos; Kyriakids, Elias; Albu, Mihaela M; have researched Uncertainty bounds of transmission line parameters estimated from synchronized measurements. The authors

listed as the transmission line parameters have a great impact on monitoring, control, and the power systems operators. Similarly, overhead transmission line parameters that are stored in the control center database are subjected to different errors. In this paper, to decrease the error installing the phasor measurement unit (PMU) at both ends of the transmission line is used. It is also used to calculate the transmission line parameters using synchronized current and voltage phasor measurements and also the uncertainty due to phasor measurement error and the instrument transformer should have been included in the calculated transmission line parameter values. The calculated bounds of uncertainty have been evaluated through MC simulations and the simulation results are obtained using the IEEE 14-bus system with many simulations due to randomness nature of the MC method [14].

However, the thesis encompasses the analysis of sag, tension, conductor length, and resistance on the Ethiopian 400kV overhead transmission line from Bahir Dar to Addis Ababa. Also, the methods used are MC and IA method for probabilistic and bounded uncertain parameters respectively and comparison of the two methods are presented.

Chapter 3

Mathematical modeling and analysis

3.1. Theory of overhead transmission line

3.1.1 Introduction

The main components of the electric power system are Generation, Transmission, and Distribution systems. In the electric power world,

Generating station and distribution systems are linked by transmission lines. Transmission lines are used to transfer the bulk power by high voltage range between main load centers and overhead lines are the backbone of the electrical power transmission [27],[36],[37].

Normally, transmission lines are categorized as underground and overhead transmission lines. The underground transmission line shown in Fig 3.2 is the way which is used to transfer electric power through underground system and overhead transmission line shown in Fig 3.1 is also the way to transfer electric power through above the ground with the help of supports/towers/poles. Both underground and overhead transmission lines have their own positive and negative impacts on the nature of voltage and the utility center. Mostly, overhead transmission lines are faced with failures because of power loss and the effect of environmental impacts compared to underground transmission lines. Above 90% of Ethiopia's electric power transmission systems are overhead transmission systems [36],[38],[39].



Figure 3.1. Overhead power transmission line (OHTL)



Figure 3.2. Underground power transmission line (UGTL)

An overhead transmission line consists of conductors and ground wires, towers, insulation, hardware, and foundations.

3.1.2 Main elements of OHTL

Due to economic considerations, a three-phase three-wire overhead system is widely used for electric power transmission. The following are the main elements of typical power systems:

- ❖ A conductor is three for a single circuit line and six for a double circuit line. It must be of proper size (i.e cross-sectional area) and depends on its current capacity [2],[40]. In this thesis, the conductor type is AAAC (all aluminum alloy conductor).
- ❖ Line insulators are used to support the line conductors while electrically isolating them from the support towers [2].
- ❖ Support towers are to support the line conductors suspending in the air overhead [2].
- ❖ Protective devices are used to protect the transmission system and to ensure reliable operation. These include ground wires, lightning arrestors, circuit breakers, relays, etc. [37].

- ❖ Voltage regulators are to keep the voltage within permissible limits at the receiving end [37].

3.1.3 The OHTL parameters

- ❖ Sag is defined as the vertical difference in level between points support (most commonly, transmission towers) and the lowest point of the conductor [2].
- ❖ Tension is defined as the erection of a transmission line (conductor) beyond the given limit [2].
- ❖ Conductor length is the length of the conductor between the supports [2].
- ❖ Span is the distance measured horizontally between two towers [2].

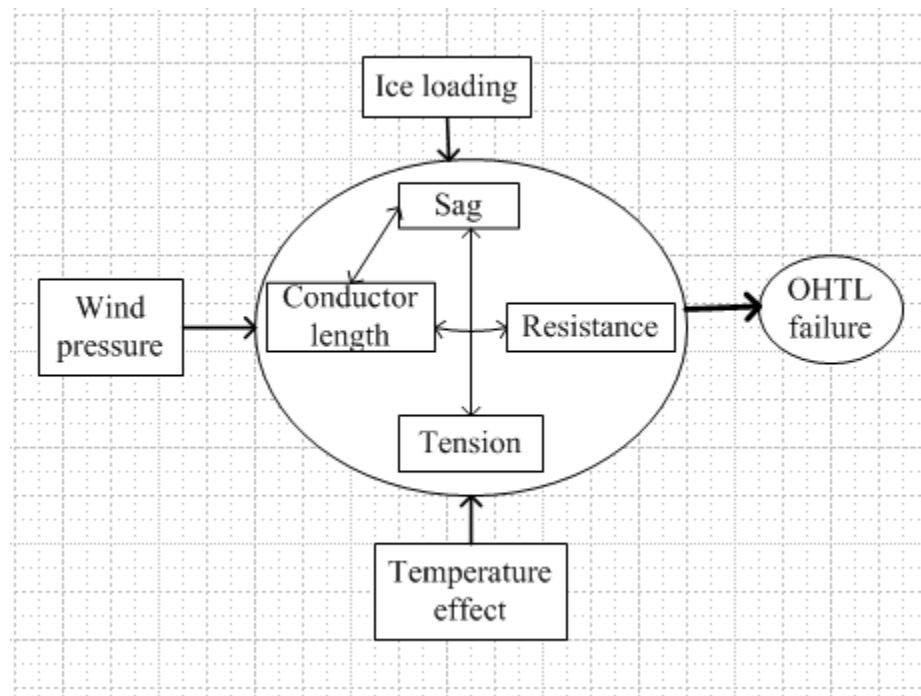


Figure 3.3. The block diagram of the factors affecting OHTL

In Fig. 3.3 the weather conditions wind pressure, temperature, and ice accumulation have a great impact on the failure of OHTL. Since overhead transmission line parameters sag, tension, conductor length and resistance tend to change with the fluctuation of weather conditions from lower to upper extremes. The decrease in sag leads to decreasing in conductor length and increasing of tension.

3.2 The effect of ice loading and wind pressure in OHTL

Wind pressure and the weight of ice on the conductor need to take into consideration while performing sag calculation for high voltage lines. The weight of the bare cable and ice loading is vertically downward from the center of the total mass. On the other hand, the wind is blowing at right angles to the line, and the net wind pressure direction is taken into the horizontal direction to the line bare cable. Therefore, the total loading of the cable, which is the result of, ice accumulation, wind pressure, and bare cable weight is based on vector summation [13], [8], [25].

Therefore, the resultant weight of the bare cable is found by using the principle of vector addition as shown in fig 3.2. The maximum effective weight of the conductor is the vector sum of the weight of the conductor and weight of ice vertically and the weight of the wind horizontally [9],[7], [35].



Figure 3.4. The effect of ice loading and wind force on OHTL

In Fig. 3.4 the overhead transmission line conductor is broken and down to the ground and covered by ice snow, the supports (towers) are also broken and down to the ground. Such type of problem has happened in the worst-case of the effect of wind pressure and ice loading effect.

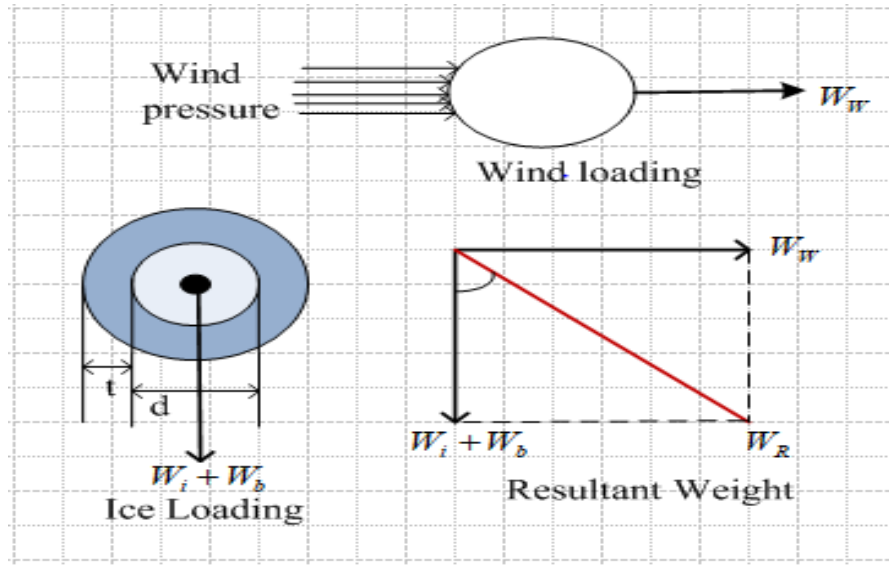


Figure 3.5. The ice, wind, and bare conductor loading on the cable and its resultant weight

Where W_R is the resultant conductor weight, W_w is the wind weight, W_b is the weight of the bare cable, $W_b + W_i$ is the sum of bare cable weight and wind weight.

To find the total loading of the cable, which is the result of, ice accumulation; wind pressure and bare cable weight are based on vector summation. The weight of the bare cable and ice loading are vertically downward from the center of the total mass. On the other hand, the wind pressure creates a horizontal force on the cable and results in a horizontal loading. The resultant weight is then found by using the principle of vector addition as shown in (3.1). In this thesis, the effect of ice loading is considered as zero.

$$\left. \begin{aligned} W_R^2 &= (W_i + W_b)^2 + W_w^2 \\ W_R &= \sqrt{(W_i + W_b)^2 + W_w^2} \\ W_R &= \sqrt{W_b^2 + W_w^2} \end{aligned} \right\} \quad (3.1)$$

$$\text{Where, } \left. \begin{aligned} W_w &= P_w \left(\frac{D_c + 2t}{12} \right), t = 0 \\ W_w &= P_w \left(\frac{D_c}{12} \right) \end{aligned} \right\} \quad (3.2)$$

The wind pressure load on any conductor can be found from (3.3), where V_{wind} is the blowing wind speed in (ft. /s). The wind pressure varies with the variation on the wind speed according to (3.3). The wind pressure load is wind pressure per unit length.

$$P_w = 0.03824(V_w^2) \quad (3.3)$$

In equation (3.1), W_R is the resultant weight, W_i is the weight of ice loading, W_b is the weight of bare conductor, and W_w is the weight of wind loading.

3.3 Catenary model of OHTL

The presence of uncertainty leads to the analysis of overhead transmission line parameters based on the unknown but bounded and probabilistic concept. [13].

Fig. 3.6 shows a conductor suspended freely from two supports, which are at the same level and spaced L meter, takes the form of a catenary curve providing the conductor is perfectly flexible and conductor weight is uniformly distributed along its length. The conductor between supports in an overhead transmission line is a catenary curve and the distribution line is a parabolic curve [41].

The starting point in the analysis is the derivation of the basic governing equation of OHTL by using a long span which is the shape of the catenary curve of the conductor as shown in fig 3.6. All the OHTL parameters, namely, resultant weight loading, conductor sag, tension, and conductor length of a catenary-shaped OHTL are developed based on fig 3.6. In the figure, it is assumed that a catenary cable is formed on a level long span with the two halves of the curve is symmetric to each other. All the basic equations for any long span OHTL with catenary shape are derived from this assumption [4],[42],[44].

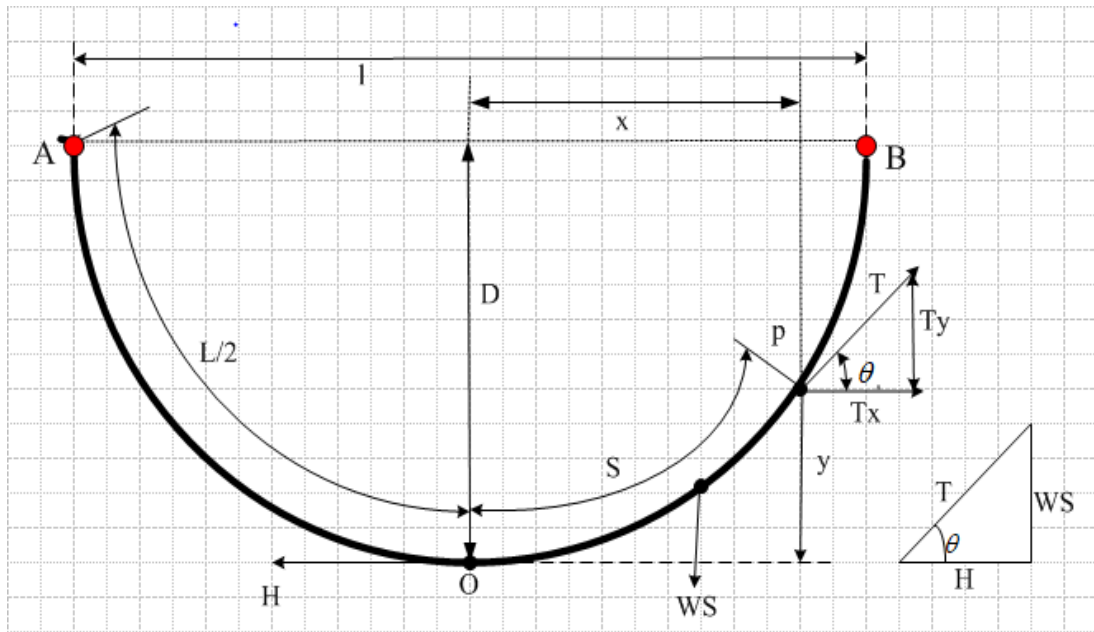


Figure 3.6. Catenary shaped conductor suspended between two supports (towers)

Where A and B are supports of the bare cable, D is the sag of the bare cable, in ft, l is the distance between the supports, in ft, L is the length of the bare cable, in ft, H is the tension at the lowest point the bare cable, in lbs, θ is the angle formed by T with the horizontal axis in degree, O is center of the cable, W is the weight of the cable per-unit length, in lbs./ft, S is the length of the bare cable measured from the lowest point of H to any point (the arc length) $p(x,y)$, in ft, and y is the vertical height of any point $p(x,y)$ as measured above the origin [4], [32].

Consider the equilibrium of the small length of the wire up to a point $p(x,y)$. The three forces acting on this length of the conductor are the horizontal tension (H), the vertical downward weight (W_s), and the tangential tension (T). T can be resolved into the horizontal and vertical components T_x and T_y respectively. Thus, the portion of the OP of the conductor is in equilibrium under the tension T at P . Under equilibrium conditions, the summation of all forces in the x -axis and y -axis is zero [41], [45].

$$\left. \begin{aligned} \sum F_x = 0, \quad H - T_x = 0, \quad T_x = H \\ \sum F_y = 0, \quad WS - T_y = 0, \quad T_y = WS \end{aligned} \right\} \quad (3.4)$$

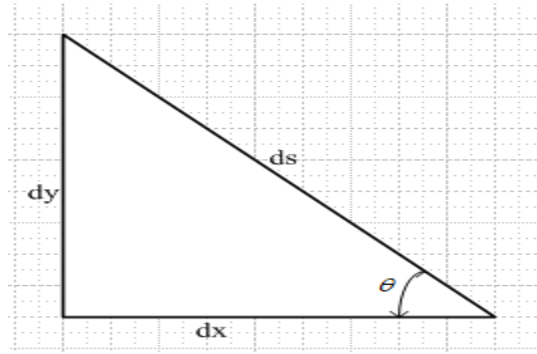


Figure 3.7. Triangle formed by the tangential and horizontal component

Fig 3.7 shows a triangle, where ds represents a very short portion of the conductor in the region of point p , d_x represents the horizontal component, and d_y represents the vertical component. When S is increased by ds , the corresponding x and y are also increased by d_x and d_y , respectively [41], [45], [46]. Then, the tangent of the angle is shown in (3.5).

$$\tan \theta = \frac{dy}{dx} = \frac{WS}{H} \quad (3.5)$$

From Fig. 3.7,

$$(ds)^2 = (dx)^2 + (dy)^2 \quad (3.6)$$

Dividing equation (3.6) both sides by $(dx)^2$,

$$\left(\frac{ds}{dx}\right)^2 = 1 + \left(\frac{dy}{dx}\right)^2 \quad (3.7)$$

Using equation (3.5) and (3.7), we get,

$$\left. \begin{aligned}
 \left(\frac{ds}{dx}\right)^2 &= 1 + \left(\frac{WS}{H}\right)^2 \\
 \frac{ds}{dx} &= \sqrt{1 + \left(\frac{WS}{H}\right)^2} \\
 dx \left(\sqrt{1 + \left(\frac{WS}{H}\right)^2}\right) &= ds \\
 dx &= \frac{ds}{\sqrt{1 + \left(\frac{WS}{H}\right)^2}}
 \end{aligned} \right\} \quad (3.8)$$

Then, integrating both sides of equation (3.8), we get

$$\begin{aligned}
 \int dx &= \int \left(\frac{ds}{\sqrt{1 + \left(\frac{WS}{H}\right)^2}}\right) \\
 x &= \int \left(\frac{ds}{\sqrt{1 + \left(\frac{WS}{H}\right)^2}}\right)
 \end{aligned} \quad (3.9)$$

Therefore, the formula for the horizontal component from equation (3.9) is

$$x = \frac{H}{W} \sinh^{-1}\left(\frac{WS}{H}\right) + k \quad (3.10)$$

Where, k is constant of integration, when $x=0$, $S=0$, and k is also =0. Then,

$$x = \frac{H}{W} \sinh^{-1}\left(\frac{WS}{H}\right) \quad (3.11)$$

The arc length S is also calculated from equation (3.11) by performing some rearrangements and given as:

$$S = \frac{H}{W} \sinh\left(\frac{Wx}{H}\right) \quad (3.12)$$

To calculate the length of bare cable substituting $x=l/2$ and $S=L/2$ in equation (3.12).

$$\left. \begin{aligned} \frac{L}{2} &= \frac{H}{W} \sinh\left(\frac{Wl}{2H}\right) \\ L &= \frac{2H}{W} \sinh\left(\frac{Wl}{2H}\right) \end{aligned} \right\} \quad (3.13)$$

Equation (3.13) also written as:

$$L = \frac{2H}{W} \left[\frac{1}{1!} \frac{Wl}{2H} + \frac{1}{3!} \left(\frac{Wl}{2H}\right)^3 + \dots \right] \quad (3.14)$$

Equation (3.14) also approximately written as:

$$\left. \begin{aligned} L &\cong l \left(1 + \frac{W_R^2 l^2}{24H^2} \right) \\ L &\cong l + \frac{W_R^2 l^3}{24H^2} \\ L &\cong l + \frac{8D^2}{3l} \end{aligned} \right\} \quad (3.15)$$

From equation (3.5) and (3.12), we get,

$$\left. \begin{aligned} \frac{d_y}{d_x} &= \frac{WS}{H} = \sinh\left(\frac{Wx}{H}\right) \\ d_y &= \sinh\left(\frac{Wx}{H}\right) d_x \end{aligned} \right\} \quad (3.16)$$

Integrating both sides of equation (3.16), we can get,

$$\left. \begin{aligned} \int d_y &= \int \sinh\left(\frac{Wx}{H}\right) d_x \\ y &= \int \sinh\left(\frac{Wx}{H}\right) d_x \\ y &= \frac{H}{W} \cosh\left(\frac{Wx}{H}\right) + K_1 \end{aligned} \right\} \quad (3.17)$$

The lowest point of the curve is taken as the origin, then the equation of the catenary is as follows:

$$y = \frac{H}{W} \left[\cosh\left(\frac{Wx}{H}\right) - 1 \right] \quad (3.18)$$

From Fig. 3.6 by the principle of Pythagorean tangential force can be calculated as:

$$\left. \begin{aligned} T &= \sqrt{H^2 + (WS)^^2} \\ T &= H \sqrt{1 + \left(\frac{WS}{H}\right)^2} \end{aligned} \right\} \quad (3.19)$$

From equation (3.19) and (3.5), we get,

$$T = H \sqrt{1 + \left(\frac{d_y}{d_x}\right)^2} \quad (3.20)$$

From equation (3.16), we can get,

$$\frac{d_y}{d_x} = \sinh\left(\frac{Wx}{H}\right) \quad (3.21)$$

From equation (3.20) and (3.21), we get,

$$T = H \cosh\left(\frac{Wx}{H}\right) \quad (3.22)$$

The total tension in the bare cable at the support (at $x=l/2$) is given as,

$$\left. \begin{aligned} T &= H \left[1 + \frac{1}{2!} \left(\frac{Wl}{2H}\right)^2 + \frac{1}{4!} \left(\frac{Wl}{2H}\right)^4 + \dots \right] \\ \text{Approximately,} \\ T &= H \cosh\left(\frac{Wl}{2H}\right) \end{aligned} \right\} \quad (3.23)$$

The sag of the bare cable for a span length of l between supports on the same level from equation (3.18) ($y=D$) can be given as,

$$\left. \begin{aligned} D &= \frac{H}{W_R} \left[\cosh \left(\frac{W_R l}{2H} \right) - 1 \right] \\ D &= \frac{l}{2} \left[\frac{1}{2} \left(\frac{W_R l}{2H} \right) + \frac{1}{4!} \left(\frac{W_R l}{2H} \right)^3 + \frac{1}{6!} \left(\frac{W_R l}{2H} \right)^5 + \dots \right] \\ \text{Approximately,} \\ D &= \frac{W_R l^2}{8H} \end{aligned} \right\} \quad (3.24)$$

3.4 Temperature change in OHTL

Temperature affects sag and stress because of the thermal expansion and contraction of the conductor. Temperature raises of the conductor increases the length of the conductor, and hence sag increases and tension decreases. Also, temperature fall causes a decrease in the length of the conductor, and sag decreases, and tension increases. It also found that the operation of the conductors at high temperatures reduces the mechanical integrity of the overhead systems and reduces transmission capacity [7], [35], [47].

Temperature affects how electricity flows through an electrical circuit by changing the speed at which the electrons travel. This is due to an increase in resistance of the circuit that results from an increase in temperature. Likewise, resistance is decreased with decreasing temperature [7], [48], [49].

3.4.1 Thermal Elongation

Heat causes conductors to expand, results in the length of the conductor becomes longer and sags higher. The distance that a particular conductor expands is often described by a linear temperature coefficient α_T [35]. The length of a simple conductor is given as:

$$L_T = (1 + \alpha_T \times (T - T_o)) L_{T_o} \quad (3.25)$$

Where L_T is the length of the cable at temperature $T(^{\circ}C)$, in ft, L_{T_0} is the length of the cable at initial temperature $T_0(^{\circ}C)$, in ft, α_T is the coefficient of thermal expansion, in $/^{\circ}C$.

3.4.2 Stress-Strain Behavior

If the conductor cables are tensioned, they will undergo deformation, and as stress increases the conductor cables undergo strain mostly at linear characteristics. This linear property is considered elastic. As stress increases as shown in Fig. 3.8, some of the strain becomes permanent. After this point, if the cable is relaxed, it will shrink linearly but will retain some deformation permanently. This permanent deformation is considered as plastic deformation [50], [51].

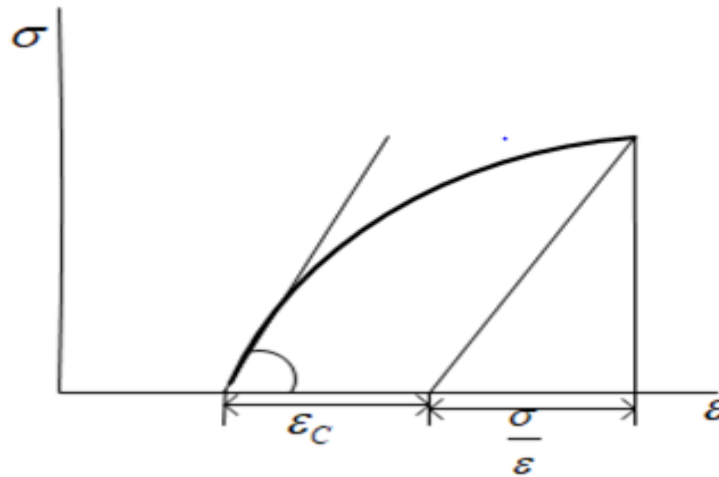


Figure 3.8. Stress-Strain relationship

The length of a conductor in its range of elastic behavior, concerning stress, σ is given as:

$$\left. \begin{aligned} L_{\sigma} &= L \times (1 + \varepsilon_{\sigma} + \varepsilon_c) \\ \varepsilon_{\sigma} &= \frac{\sigma}{E} = \frac{H}{EA} \end{aligned} \right\} \quad (3.26)$$

In equation (3.26), L_σ is the length under stress σ , in ft., L is the length under no stress, in ft., ε_σ is an elastic strain, σ is stress, in $\frac{lb}{in^2}$, E is the modulus of elasticity for the conductor, in $\frac{lb}{in^2}$, A cross-sectional area, in in^2 , H is the tension applied to the conductor, in lbs , ε_c is the plastic deformation of the cable, due to inelastic deformation and creep.

If conductor stress is constant while the temperature changes, the change in length of the conductor is shown in Fig. 3.8.

$$\left. \begin{aligned} \Delta l &= l_o \alpha \Delta t \\ \text{Where, } \Delta t &= t_1 - t_o \\ \Delta l &= l_1 - l_o \end{aligned} \right\} \quad (3.27)$$

In equation (3.27), t_o is initial temperature, l_o is conductor length at the initial temperature t_o , l_1 is the conductor length at t_1 , α its coefficient of linear expansion of conductor per degree centigrade, Δt is a temperature change and Δl is the change in conductor length.

If the temperature is constant while the conductor stress changes (loading), the change in length of the conductor is:

$$\left. \begin{aligned} \Delta l &= l_o \cdot \frac{\Delta T}{MA} \\ \text{Where, } \Delta T &= T - T_o \end{aligned} \right\} \quad (3.28)$$

Equation (3.28) contains, T_o is initial tension of the bare cable in-lb, ΔT is the change in the bare cable tension in lb, M modulus of elasticity of the bare cable in lb/ft, and A is the actual metal cross-section of the conductor in ft^2 .

The length of the cable increases while the span remains the same when the line undergoes thermal expansion. This particular effect may result in a decrease in tension in

the conductor. In this scenario to find the sag of a given span, both thermal expansion and elastic elongation with loading must be considered together. To find the sag, we must find a tension H at which the length of the elongated cable is equal to the catenary cable length. The conductor length change due to thermal expansion and elastic elongation combined is given by (3.31).

$$L = L_o \left(1 + \alpha_T (T - T_o)\right) \left(1 + \frac{H - H_o}{EA} + e_c\right) \quad (3.29)$$

Where L is the length at high-temperature conditions, in ft, Lo is initial length, in ft, Ho is initial tension, in lbs., To is the stringing temperature, in degree centigrade.

Substitute the linear approximation of cable length, from equation (3.15) to equation (3.29), is given:

$$l + \frac{W_R^2 l^3}{24H^2} = \left(l + \frac{W_R^2 l^3}{24H_o^2}\right) \left(1 + \alpha_T (T - T_o)\right) \left(1 + \frac{H - H_o}{EA} + e_c\right) \quad (3.30)$$

Equation (3.30) can be solved to calculate horizontal tension H, which is used to calculate the sag and conductor length.

Horizontal tension H can be solved by a root-finding mechanism of cubic polynomial function which is multiplied by H^2 and rearranges as a polynomial. The coefficients k_1 , k_2 , k_3 and k_4 are given by (3.32). The cubic function in (3.31) is used to find the final tension value after different loading. Among the three roots of (3.31), only one is real and represents the final tension value. For a catenary-shaped overhead transmission line, the tension T is the same as the horizontal tension H.

$$k_1 H^3 + k_2 H^2 + k_3 H - k_4 = 0 \quad (3.31)$$

$$\left. \begin{aligned} k_1 &= \left(1 + \frac{W_R^2 l^2}{24H_o^2}\right) (1 + \alpha_T (T - T_o)) \left(\frac{1}{EA}\right) \\ k_2 &= \left(1 + \frac{W_R^2 l^2}{24H_o^2}\right) (1 + \alpha_T (T - T_o)) \left(1 - \frac{H_o}{EA} + \varepsilon_c\right) - 1 \\ k_3 &= 0 \\ k_4 &= \frac{W_R^2 l^2}{24H_o^2} \end{aligned} \right\} \quad (3.32)$$

Once the tension is found using (3.32) the next step is finding the sag and conductor length of the overhead transmission line using the equations (3.24) and (3.15) respectively. The elongation of the ASCR and AAAC conductors with the change of temperature has effects on the sag-tension characteristics. Since the rate of the steel strands expansion in ASCR conductor is half of the aluminum, the composite ASCR conductor rate of expansion is less than that of AAAC[1]. The sag, tension, and conductor length calculation using a catenary-shaped OHTL are formulated with few assumptions. The linear thermal expansion of a non-homogenous Drake ASCR conductor is found from equation (3.33) and (3.34).

$$E_{AS} = E_A \left(\frac{A_A}{A_{AS}}\right) + E_S \left(\frac{A_S}{A_{AS}}\right). \quad (3.33)$$

$$\alpha_{AS} = \alpha_A \left(\frac{E_A}{E_{AS}}\right) \left(\frac{A_A}{A_{AS}}\right) + \alpha_S \left(\frac{E_S}{E_{AS}}\right) \left(\frac{A_S}{A_{AS}}\right) \quad (3.34)$$

Where E_A is the elastic modulus of aluminum (psi), E_S is the elastic modulus of steel (psi), E_{AS} is the elastic modulus of aluminum-steel composite (psi), A_A is an area of aluminum strands, (su), A_S is the area of steel strands (su), A_{AS} is the total cross-sectional area (su), α_A is the aluminum coefficient of linear thermal expansion (per $^{\circ}\text{F}$), α_S is steel coefficient of thermal elongation (per $^{\circ}\text{F}$) and α_{AS} is composite aluminum-steel coefficient of thermal elongation (per $^{\circ}\text{F}$). AAAC is a homogeneous conductor. Alloy aluminum facilitate current carrying as well as mechanical strength to the conductor. Its current carrying capacity is slightly higher compared to ACSR conductor. But alloy

aluminum conductors are not heat treated. Therefore they can not operated at higher temperature[9].

3.5 Interval Arithmetic approach

During the 1960s a new approach, known as interval analysis, emerged as an alternative way of dealing with uncertainty in data. In a mathematical model under study using a single floating-point number does not perfectly represent the exact value of the variables

Since uncertainty is a major issue facing electric utilities and the value of overhead transmission line parameters sag, tension, and the length of the cable. It is no longer valid to assume that the input and output parameters of OHTL are known with certainty [9], [28]. The concept of uncertainty can be based on two general approaches. The first is the Unknown but bounded approach in which the upper and lower limits on the uncertainty are assumed without a probability distribution.

The second approach is probabilistic where probability distributions for all of the uncertainties are assumed [12], [23].

To implement and extend unknown but bounded concept interval analysis method is a very essential concept and also it is a useful tool in determining the effect of uncertainty in parameters used in a computation. By using interval analysis, there is no need for many simulations run because the total variation in the output is known given the total variation in input parameters. Interval analysis used interval numbers instead of ordinary single point numbers. An Interval number is an ordered pair of real numbers representing the lower and upper bounds of the parameter range and defined as: $[a,b]$, where $a \leq b$ [23], [16], [52].

Given two numbers, $[a, b]$ and $[c, d]$, the rule for interval analysis for addition, subtraction, multiplication, and division are given as follows [28]:

$$\text{Interval addition, } [a, b] + [c, d] = [a+c, b+d]$$

$$\text{Interval subtraction, } [a, b] - [c, d] = [a-d, b-c]$$

$$\text{Interval multiplication, } [a, b] * [c, d] = [\min(ac, ad, bc, bd), \max(ac, ad, bc, bd)]$$

Interval division, $[a, b] / [c, d] = [a, b] * [1/d, 1/c]$, where $0 \neq [c, d]$.

The sag and conductor length of an overhead transmission line is affected by loading, heating and long term creep. As result, the sag from the lower limit D_o to the upper limit D and the tension is from lower limit H_o to upper limit H according to (3.34), and also the conductor length from the lower limit L_o to upper limit L according to (3.35). The length of the cable increases while the span remains the same when the line undergoes thermal expansion. This particular effect may result in a decrease in tension in the conductor [9], [19].

$$\left. \begin{aligned} D &= \frac{W_R l^2}{8H} \\ D_o &= \frac{W_R l^2}{8H_o} \end{aligned} \right\} \quad (3.34)$$

$$\left. \begin{aligned} L &= l + \frac{8D^2}{3l} \\ L_o &= l + \frac{8D_o^2}{3l} \end{aligned} \right\} \quad (3.35)$$

3.6 Monte Carlo approach

The Monte Carlo approach is developed by Stan Ulam in 1940. The Monte Carlo method is a class of numerical methods that relies on random sampling and is based on the idea of taking a small, randomly-drawn sample from a population and estimating the desired outputs from the given sample. The MC method requires three steps, the first is generating a random sample of the input parameters according to the distributions of the inputs, the second is analyzing each set of the inputs in the sample and the third is estimating the desired probabilistic outputs, and the uncertainty in these outputs using the random sample. The probabilistic distribution approach of uncertainty can be implemented by MC analysis [17], [53], [54].

In mathematical modeling of a given system, the final and the intermediate expression of the system may end up with no analytical solution. The Monte Carlo method is the numerical method that uses a random number. For continuous random variables, the random variables which can assume any value within some defined range, the PDF expresses the probability that the random variable falls within some very small interval. For discrete random variables, that can only assume certain isolated or fixed values, the term probability mass function (PMF) is preferred over the term PDF. PMF expresses the probability that the random variable takes on a specific value. In the context of MC simulation, simulation is the process of approximating the output of a model through repetitive random application of a model's algorithm [17], [54], [55].

A continuous random variable 'z' can take any value in the bounded interval [a, b]. Then the probability of z being in an arbitrary interval [a', b'] is defined by a pdf as in (3.36)

$$\left. \begin{aligned}
 P(a' \leq z \leq b') &= \int_{a'}^{b'} P(z) dz \\
 \text{subject ed to :} \\
 1) \quad P(z) &\geq 0 \text{ for any } z \in [a, b] \\
 2) \quad \int_a^b P(z) dz &= 1
 \end{aligned} \right\} \quad (3.36)$$

The expected value is shown in (3.37). In a digital computer, if the random number generator only generates a random number R(n) between the interval [0, 1], then true random number R_t(n) in the real interval [a, b] can be found by using (3.38) [54].

The expected value of the random variable becomes:

$$E(z) = \int_a^b z P(z) dz \quad (3.37)$$

$$R_t(n) = R(n)(b - a) + a \quad (3.38)$$

where 'n' is the number of random variables, a is the lower bound of the interval and 'b' is the upper bound of the interval.

Uncertainty refers to someone who is not perfect about something because of different uncontrollable factors like weather change. A random variable is a quantity that can take on any number of values but whose exact value cannot be known before a discrete observation is made [53].

3.7 Case Study area of the thesis

To validate the proposed IA and MC based OHTL parameter calculation, with input uncertainty, a 400kV (Bahir Dar-Debre Markos-Addis Ababa) OHTL and a test case containing temperature and wind speed variations for 10 cities which are the worst cases are used. The type of conductor used is all aluminum alloy conductor (AAAC). The 400kV OHTL crosses many cities and towns which are around 20 or above and the analysis is done for the worst-case 10 cities.

The collected data for this thesis is 5 years of temperature and wind speed from 2013-2017 G.C for 10 cities and installed data of 400kV OHTL from Bahirdar to Addis Ababa. The daily data of temperature and wind speed are collected from NASA and the metrology agency of the northern region Bahir Dar district. In this thesis, the initial horizontal tension and span length are taken from EEPU northwest region bahirdar district of 400kv overhead transmission line as shown in appendix B..

The name of selected cities for the analysis purpose is listed as Bahr Dar, Dangila, Enjibara, Bura, Finote Selam, Debre markos, Dejen, Gerb Gurach, Ficha, and Addis Abeba. It is selected based on the worst input uncertain of wind speed and temperature change.

Chapter 4

Results and conclusion

4.1 Results

4.1.1 OHTL parameters of Bahir Dar city

Table 4.1. Initial inputs and resistance of Bahir Dar

Uncertain input parameters			Resistance change with temperature (Ω/m)	
Month	Wind speed (m/s)	Temperature ($^{\circ}C$)	RDC	RAC
Jan	[3.4400 4.0300]	[18.8123 20.3058]	[0.1030 0.1036]	[0.1542 0.1551]
Feb	[3.7400 4.2300]	[20.7618 22.2539]	[0.1021 0.1027]	[0.1530 0.1539]
Mar	[3.5700 4.0900]	[22.2819 24.2323]	[0.1012 0.1021]	[0.1521 0.1530]
Apr	[3.6900 4.0700]	[22.8987 24.5437]	[0.1009 0.1018]	[0.1518 0.1527]
May	[3.1000 4.0300]	[21.0223 22.5381]	[0.1018 0.1024]	[0.1530 0.1536]
Jun	[3.5500 3.9600]	[19.6737 20.9887]	[0.1027 0.1033]	[0.1539 0.1545]
Jul	[3.2600 3.7300]	[17.3423 19.4068]	[0.1033 0.1042]	[0.1545 0.1558]
Aug	[3.0700 3.5400]	[17.4694 18.7332]	[0.1036 0.1042]	[0.1551 0.1558]
Sep	[2.9400 3.3200]	[18.6860 19.7183]	[0.1030 0.1036]	[0.1545 0.1551]
Oct	[3.1900 3.5600]	[18.6777 19.8481]	[0.1030 0.1036]	[0.1545 0.1551]
Nov	[3.1900 3.5600]	[18.2570 19.1147]	[0.1033 0.1039]	[0.1548 0.1554]
Dec	[3.2000 4.0200]	[17.9190 24.5437]	[0.1009 0.1039]	[0.1518 0.1554]

Table 4.2. Sag and conductor length of Bahirdar

Month	Sag change (m)		Conductor length change (m)	
	DIA	DMC	LIA	LMC

Worst-case Analysis of OHTL Parameters with Uncertainty using IA and MC approach

Jan	[3.5895 4.0776]	[3.7452 3.9081]	[123.6210 123.7020]	[123.6452 123.6721]
Feb	[3.6605 4.1560]	[3.8186 3.9839]	[123.6322 123.7159]	[123.6572 123.6850]
Mar	[3.6269 4.0904]	[3.7751 3.9298]	[123.6269 123.7042]	[123.6501 123.6757]
Apr	[3.6928 4.0411]	[3.8054 3.9216]	[123.6373 123.6956]	[123.6550 123.6743]
May	[3.4622 4.1537]	[3.6787 3.9093]	[123.6016 123.7155]	[123.6346 123.6723]
Jun	[3.6705 3.9743]	[3.7690 3.8704]	[123.6337 123.6840]	[123.6491 123.6658]
Jul	[3.6031 3.9273]	[3.7080 3.8162]	[123.6231 123.6759]	[123.6392 123.6568]
Aug	[3.5828 3.8617]	[3.6734 3.7664]	[123.6200 123.6649]	[123.6337 123.6487]
Sep	[3.5915 3.7826]	[3.6541 3.7179]	[123.6213 123.6518]	[123.6307 123.6408]
Oct	[3.6163 3.8536]	[3.6937 3.7729]	[123.6252 123.6635]	[123.6369 123.6497]
Nov	[3.6184 3.8508]	[3.6942 3.7718]	[123.6255 123.6631]	[123.6370 123.6495]
Dec	[3.4363 4.2893]	[3.6997 3.9838]	[123.5978 123.7402]	[123.6379 123.6850]

Table 4.3. Resultant weight, tension, and resistance of Bahirdar

Month	Resultant weight change (kg /m)	Tension change (N)	Resistance change with the length of the conductor (Ω)	
	WRIA	HIA	RDC	RAC
Jan	[22.1941 23.1569]	[10032 9952]	[0.0137 0.0138]	[0.0205 0.0206]
Feb	[22.6275 23.6049]	[10016 9933]	[0.0136 0.0137]	[0.0204 0.0205]
Mar	[22.3696 23.2843]	[9890 9828]	[0.0134 0.0136]	[0.0202 0.0204]
Apr	[22.5490 23.2373]	[9870 9831]	[0.0134 0.0135]	[0.0202 0.0203]
May	[21.8010 23.1637]	[9940 9790]	[0.0135 0.0137]	[0.0203 0.0205]
Jun	[22.3343 22.9333]	[9970 9935]	[0.0136 0.0137]	[0.0205 0.0206]
Jul	[21.9735 22.6137]	[9990 9984]	[0.0137 0.0139]	[0.0206 0.0207]
Aug	[21.7696 22.3196]	[9975 9946]	[0.0138 0.0139]	[0.0206 0.0207]
Sep	[21.6549 22.0324]	[9886 9871]	[0.0137 0.0138]	[0.0206 0.0206]
Oct	[21.8892 22.3578]	[9931 9910]	[0.0137 0.0138]	[0.0205 0.0206]
Nov	[21.8931 22.3510]	[9963 9929]	[0.0138 0.0138]	[0.0206 0.0207]
Dec	[21.9245 23.6049]	[9950 9925]	[0.0134 0.0139]	[0.0202 0.0207]

Where R DC is Dc resistance, R AC is AC resistance, DIA is a sag by IA, DMC is a sag

by MC, LIA conductor length by IA, LMC is conductor length by MC, HIA horizontal tension. by IA, and WRIA is resultant weight by IA.

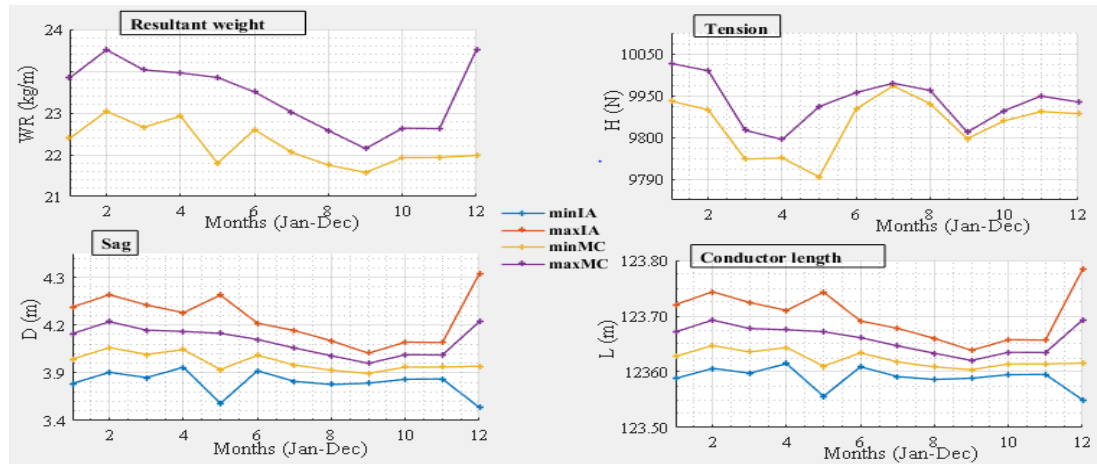


Figure 4.1. OHTL parameters variation for Bahirdar city

4.1.2 OHTL parameters of Dangila city

Table 4.4. Initial inputs and resistance of Dangila

Month	Uncertain input parameters		Resistance change with temperature (Ω/m)	
	Wind speed (m/s)	Temperature ($^{\circ}C$)	RDC	RAC
Jan	[3.5500 4.1900]	[17.6368 19.6129]	[0.1033 0.1042]	[0.1545 0.1558]
Feb	[3.9400 4.5300]	[20.1739 21.9475]	[0.1021 0.1030]	[0.1533 0.1542]
Mar	[3.6300 4.3800]	[21.8203 23.7445]	[0.1012 0.1021]	[0.1521 0.1533]
Apr	[3.4100 4.2900]	[22.1047 24.3883]	[0.1009 0.1021]	[0.1518 0.1530]
May	[2.9100 3.6600]	[20.0019 21.5681]	[0.1024 0.1030]	[0.1533 0.1542]
Jun	[2.9200 3.5400]	[18.8083 19.8290]	[0.1030 0.1036]	[0.1545 0.1551]
Jul	[2.8800 3.2600]	[16.8877 18.4768]	[0.1036 0.1045]	[0.1551 0.1561]
Aug	[2.8300 3.3800]	[16.9810 18.1510]	[0.1039 0.1045]	[0.1554 0.1561]
Sep	[2.8200 3.0600]	[17.8517 18.6447]	[0.1036 0.1039]	[0.1551 0.1554]
Oct	[3.0000 3.3800]	[17.9561 18.8013]	[0.1036 0.1039]	[0.1551 0.1554]
Nov	[3.0700 3.3600]	[17.4097 18.0590]	[0.1039 0.1042]	[0.1554 0.1558]
Dec	[3.1600 3.680]	[17.0181 23.6484]	[0.1012 0.1045]	[0.1524 0.1561]

Table 4.5. Sag and conductor length of Dangila

Month	Sag change (m)		Conductor length change (m)	
	DIA	DMC	LIA	LMC
Jan	[3.5895 4.0776]	[3.7697 3.9667]	[123.6200 123.7191]	[123.6492 123.6820]
Feb	[3.6605 4.1560]	[3.8792 4.1094]	[123.6325 123.7520]	[123.6672 123.7068]
Mar	[3.6269 4.0904]	[3.7897 4.0429]	[123.6154 123.7445]	[123.6524 123.6952]
Apr	[3.6928 4.0411]	[3.7376 4.0056]	[123.6055 123.7408]	[123.6440 123.6887]
May	[3.4622 4.1537]	[3.6499 3.7975]	[123.6086 123.6799]	[123.6300 123.6537]
Jun	[3.6705 3.9743]	[3.6513 3.7673]	[123.6133 123.6691]	[123.6302 123.6488]
Jul	[3.6031 3.9273]	[3.6458 3.7071]	[123.6205 123.6496]	[123.6294 123.6391]
Aug	[3.5828 3.8617]	[3.6393 3.7311]	[123.6149 123.6588]	[123.6284 123.6430]
Sep	[3.5915 3.7826]	[3.6381 3.6722]	[123.6234 123.6395]	[123.6282 123.6335]
Oct	[3.6163 3.8536]	[3.6629 3.7312]	[123.6220 123.6548]	[123.6321 123.6430]
Nov	[3.6184 3.8508]	[3.6738 3.7270]	[123.6260 123.6515]	[123.6338 123.6423]
Dec	[3.4363 4.2893]	[3.6888 3.8027]	[123.6194 123.6747]	[123.6362 123.6546]

Table 4.6. Resultant weight, tension, and resistance of Dangila

Month	Resultant weight change (kg /m)	Tension change (N)	Resistance change with the length of the conductor (Ω)	
	WRIA	HIA	RDC	RAC
Jan	[22.3382 23.5029]	[10110 10027]	[0.0137 0.0139]	[0.0206 0.0207]
Feb	[22.9853 24.3451]	[10132 10012]	[0.0136 0.0137]	[0.0204 0.0205]
Mar	[22.4569 23.9529]	[10007 9861]	[0.0135 0.0136]	[0.0203 0.0204]
Apr	[22.1490 23.7343]	[9950 9800]	[0.0134 0.0136]	[0.0202 0.0204]
May	[21.6304 22.5029]	[9879 9808]	[0.0136 0.0137]	[0.0204 0.0205]
Jun	[21.6392 22.3245]	[9927 9863]	[0.0137 0.0138]	[0.0205 0.0206]
Jul	[21.6069 21.9686]	[9948 9931]	[0.0138 0.0139]	[0.0207 0.0208]
Aug	[21.5686 22.1108]	[9968 9937]	[0.0138 0.0139]	[0.0207 0.0208]
Sep	[21.5608 21.7627]	[9895 9891]	[0.0138 0.0138]	[0.0206 0.0207]
Oct	[21.7069 22.1108]	[9939 9914]	[0.0138 0.0138]	[0.0206 0.0207]
Nov	[21.7716 22.0873]	[9969 9949]	[0.0138 0.0139]	[0.0207 0.0207]
Dec	[21.8608 22.5333]	[9981 9797]	[0.0135 0.0139]	[0.0203 0.0208]

Worst-case Analysis of OHTL Parameters with Uncertainty using IA and MC approach

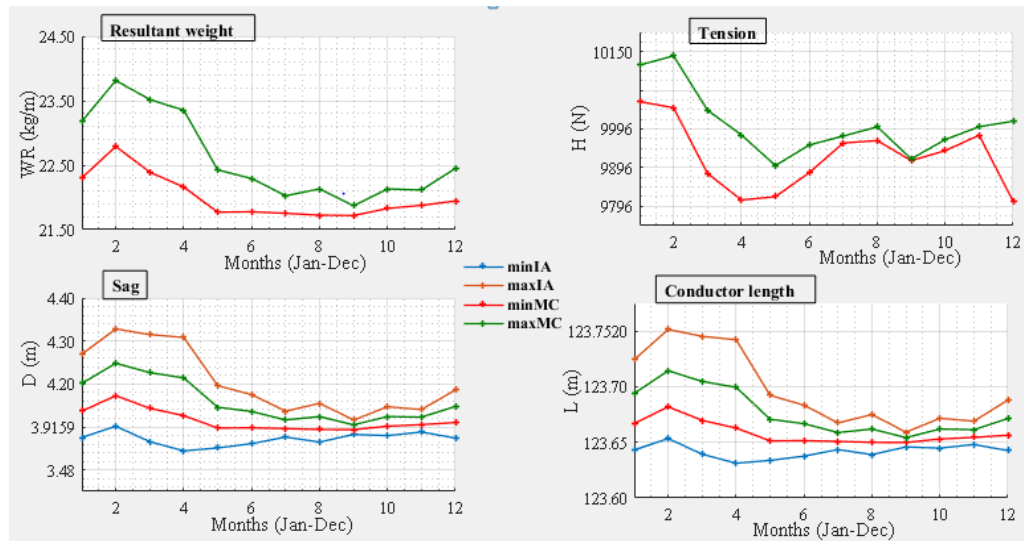


Figure 4.2. OHTL parameters variation for Dangila city

4.1.3 OHTL parameters of Enjibara city

Table 4.7. Initial inputs and resistance of Enjibara

Month	Uncertain parameters		Resistance change with temperature (Ω/m)	
	Wind speed (N/m)	Temperature ($^{\circ}C$)	RDC	RAC
Jan	[3.4200 4.1700]	[18.0200 20.0000]	[0.1030 0.1039]	[0.1542 0.1554]
Feb	[3.6000 4.3800]	[20.5600 22.3500]	[0.1018 0.1027]	[0.1530 0.1539]
Mar	[3.3100 4.2900]	[22.1400 23.8000]	[0.1012 0.1021]	[0.1521 0.1530]
Apr	[3.0700 4.2100]	[21.8900 24.5900]	[0.1009 0.1021]	[0.1518 0.1533]
May	[2.7700 3.3400]	[19.7800 21.2000]	[0.1024 0.1030]	[0.1536 0.1545]
Jun	[2.8000 3.2500]	[18.7300 19.8600]	[0.1030 0.1036]	[0.1545 0.1551]
Jul	[2.7200 3.1300]	[16.8800 18.4300]	[0.1036 0.1045]	[0.1551 0.1561]
Aug	[2.6800 3.2000]	[17.0200 18.1000]	[0.1039 0.1045]	[0.1554 0.1561]
Sep	[2.5400 2.7900]	[17.9300 18.6600]	[0.1036 0.1039]	[0.1551 0.1554]
Oct	[2.6800 3.4000]	[18.1000 18.8700]	[0.1036 0.1039]	[0.1548 0.1554]
Nov	[2.9700 3.3900]	[17.2100 18.1200]	[0.1039 0.1042]	[0.1554 0.1561]
Dec	[3.0100 3.6800]	[17.0700 17.6500]	[0.1042 0.1045]	[0.1558 0.1561]

Table 4.8. Sag and conductor length of Enjibara

Month	Sag change (m)		Conductor length change (m)	
	DIA	DMC	LIA	LMC
Jan	[3.5895 4.0776]	[3.7398 3.9592]	[123.6124 123.7222]	[123.6443 123.6807]
Feb	[3.6605 4.1560]	[3.7820 4.0429]	[123.6132 123.7462]	[123.6512 123.6952]
Mar	[3.6269 4.0904]	[3.7168 4.0057]	[123.5997 123.7452]	[123.6406 123.6887]
Apr	[3.6928 4.0411]	[3.6738 3.9742]	[123.5919 123.7420]	[123.6338 123.6833]
May	[3.4622 4.1537]	[3.6319 3.7229]	[123.6139 123.6573]	[123.6272 123.6416]
Jun	[3.6705 3.9743]	[3.6356 3.7052]	[123.6176 123.6507]	[123.6278 123.6388]
Jul	[3.6031 3.9273]	[3.6261 3.6836]	[123.6180 123.6452]	[123.6263 123.6354]
Aug	[3.5828 3.8617]	[3.6217 3.6959]	[123.6148 123.6500]	[123.6256 123.6373]
Sep	[3.5915 3.7826]	[3.6077 3.6344]	[123.6198 123.6323]	[123.6234 123.6276]
Oct	[3.6163 3.8536]	[3.6217 3.7354]	[123.6091 123.6633]	[123.6256 123.6436]
Nov	[3.6184 3.8508]	[3.6584 3.7333]	[123.6204 123.6562]	[123.6314 123.6433]
Dec	[3.4363 4.2893]	[3.6644 3.8028]	[123.6121 123.6791]	[123.6323 123.6546]

Table 4.9. Resultant weight, tension, and resistance of Enjibara

Month	Resultant weight change (kg /m)	Tension change (N)	Resistance change with the length of the conductor (Ω)	
	WRIA	HIA	RDC	RAC
Jan	[22.1618 23.4588]	[10088 9982]	[0.0137 0.0138]	[0.0205 0.0207]
Feb	[22.4108 23.9529]	[10062 9908]	[0.0136 0.0137]	[0.0204 0.0205]
Mar	[22.0255 23.7343]	[9973 9778]	[0.0135 0.0136]	[0.0202 0.0204]
Apr	[21.7716 23.5480]	[9915 9747]	[0.0134 0.0136]	[0.0202 0.0204]
May	[21.5245 22.0618]	[9825 9800]	[0.0136 0.0137]	[0.0204 0.0206]
Jun	[21.5461 21.9578]	[9867 9852]	[0.0137 0.0138]	[0.0205 0.0206]
Jul	[21.4902 21.8304]	[9929 9911]	[0.0138 0.0139]	[0.0207 0.0208]
Aug	[21.4637 21.9020]	[9938 9918]	[0.0138 0.0139]	[0.0207 0.0208]
Sep	[21.3814 21.5392]	[9862 9854]	[0.0138 0.0138]	[0.0206 0.0207]
Oct	[21.4637 22.1363]	[9940 9867]	[0.0138 0.0138]	[0.0206 0.0207]
Nov	[21.6814 22.1245]	[9972 9944]	[0.0138 0.0139]	[0.0207 0.0208]
Dec	[21.7157 22.5333]	[10055 9956]	[0.0139 0.0139]	[0.0207 0.0208]

Worst-case Analysis of OHTL Parameters with Uncertainty using IA and MC approach

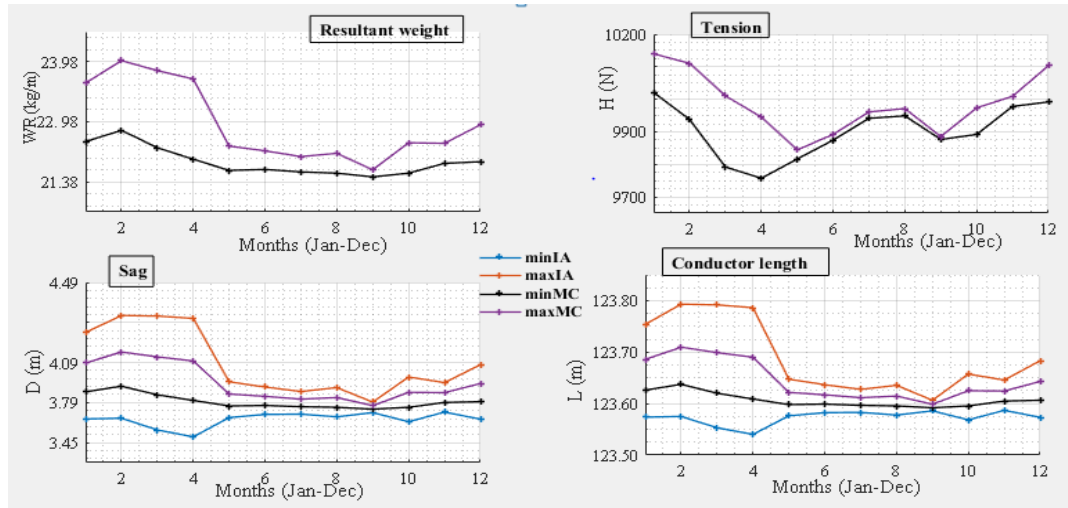


Figure 4.3. OHTL parameters variation for Enjibara city

4.1.4 OHTL parameters of Bura city

Table 4.10. Initial inputs and resistance of Bura

Month	Uncertain parameters		Resistance change with temperature (Ω/m)	
	Wind speed (m/s)	Temperature ($^{\circ}C$)	RDC	RAC
Jan	[2.0900 2.6500]	[16.3900 18.0300]	[0.1039 0.1049]	[0.1554 0.1564]
Feb	[2.0000 2.7000]	[18.4500 20.2200]	[0.1030 0.1036]	[0.1542 0.1551]
Mar	[2.0500 2.6400]	[20.2700 21.7900]	[0.1021 0.1030]	[0.1533 0.1542]
Apr	[2.0500 2.6800]	[20.1600 22.4300]	[0.1018 0.1030]	[0.1530 0.1542]
May	[1.7800 2.3000]	[18.4400 19.8700]	[0.1030 0.1036]	[0.1545 0.1551]
Jun	[1.8900 2.2400]	[17.4300 18.9000]	[0.1036 0.1042]	[0.1548 0.1558]
Jul	[1.6200 1.9500]	[15.4800 17.2500]	[0.1042 0.1052]	[0.1558 0.1570]
Aug	[1.5700 1.8100]	[15.6600 16.6600]	[0.1045 0.1052]	[0.1564 0.1567]
Sep	[1.5900 1.7400]	[16.5000 17.1800]	[0.1042 0.1045]	[0.1561 0.1564]
Oct	[1.7700 2.1900]	[16.3600 17.1500]	[0.1042 0.1049]	[0.1561 0.1564]
Nov	[1.8800 2.0900]	[15.4300 16.5300]	[0.1045 0.1052]	[0.1564 0.1570]
Dec	[1.9400 2.4000]	[15.2900 16.3000]	[0.1049 0.1052]	[0.1564 0.1570]

Table 4.11. Sag and conductor length of Bura

Month	Sag change (m)		Conductor length change (m)	
	DIA	DMC	LIA	LMC
Jan	[3.5334 3.6618]	[3.5334 3.6618]	[123.6124 123.6324]	[123.6185 123.6251]
Feb	[3.5195 3.6772]	[3.5195 3.6772]	[123.6103 123.6348]	[123.6178 123.6259]
Mar	[3.5304 3.6617]	[3.5304 3.6617]	[123.6120 123.6324]	[123.6181 123.6249]
Apr	[3.5263 3.6703]	[3.5263 3.6703]	[123.6113 123.6337]	[123.6181 123.6256]
May	[3.5374 3.6140]	[3.5374 3.6140]	[123.6130 123.6248]	[123.6165 123.6204]
Jun	[3.5490 3.6021]	[3.5490 3.6021]	[123.6148 123.6230]	[123.6171 123.6198]
Jul	[3.5475 3.5799]	[3.5475 3.5799]	[123.6145 123.6195]	[123.6158 123.6174]
Aug	[3.5504 3.5704]	[3.5504 3.5704]	[123.6150 123.6181]	[123.6156 123.6166]
Sep	[3.5536 3.5655]	[3.5536 3.5655]	[123.6155 123.6173]	[123.6157 123.6163]
Oct	[3.5437 3.6001]	[3.5437 3.6001]	[123.6140 123.6227]	[123.6164 123.6193]
Nov	[3.5569 3.5851]	[3.5569 3.5851]	[123.6160 123.6204]	[123.6170 123.6185]
Dec	[3.5418 3.6229]	[3.5418 3.6229]	[123.6137 123.6262]	[123.6174 123.6216]

Table 4.12. Resultant weight and tension of Bura

Month	Resultant weight change (kg /m)	Tension change (N)	Resistance change with the length of the conductor (Ω)	
	WRIA	HIA	RDC	RAC
Jan	[21.1912 21.4451]	[9903.9 9867.4]	[0.0138 0.0139]	[0.0207 0.0208]
Feb	[21.1657 21.4765]	[9801.2 9772.3]	[0.0137 0.0138]	[0.0205 0.0207]
Mar	[21.1784 21.4382]	[9719.3 9695.3]	[0.0136 0.0137]	[0.0204 0.0205]
Apr	[21.1804 21.4637]	[9724.2 9671.7]	[0.0136 0.0137]	[0.0204 0.0205]
May	[21.1147 21.2667]	[9793.2 9752.7]	[0.0137 0.0138]	[0.0205 0.0207]
Jun	[21.1373 21.2431]	[9844.8 9793.2]	[0.0138 0.0139]	[0.0206 0.0207]
Jul	[21.0882 21.1520]	[9931.0 9855.9]	[0.0139 0.0140]	[0.0207 0.0209]
Aug	[21.0814 21.1206]	[9921.3 9879.0]	[0.0139 0.0140]	[0.0208 0.0209]
Sep	[21.0843 21.1069]	[9880.8 9851.9]	[0.0139 0.0139]	[0.0207 0.0208]
Oct	[21.1137 21.2245]	[9892.4 9872.8]	[0.0139 0.0139]	[0.0208 0.0208]
Nov	[21.1363 21.1912]	[9941.3 9896.8]	[0.0139 0.0140]	[0.0208 0.0209]
Dec	[21.1500 21.3108]	[9950.6 9927.5]	[0.0139 0.0140]	[0.0208 0.0209]

Worst-case Analysis of OHTL Parameters with Uncertainty using IA and MC approach

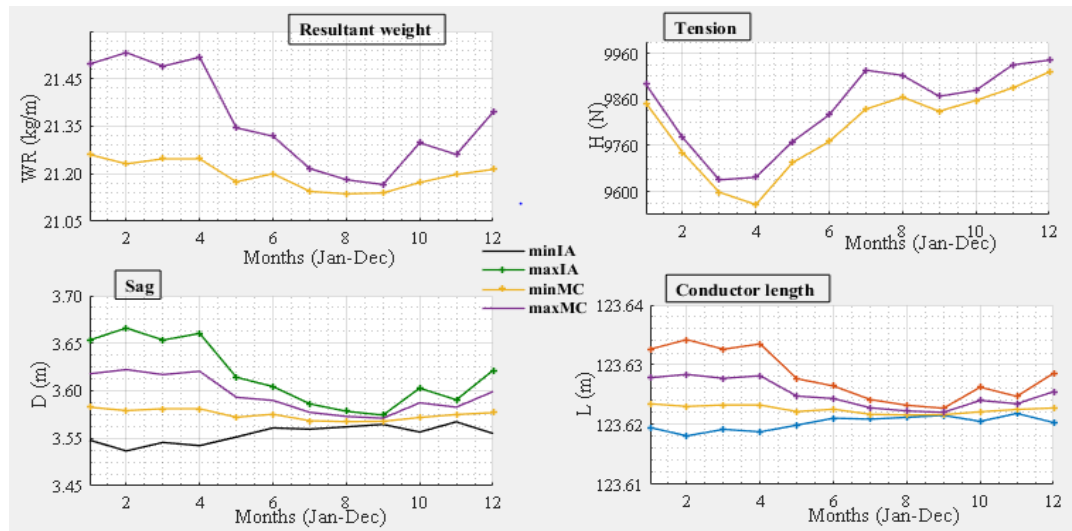


Figure 4.4. OHTL parameters variation for Bura city

4.1.5 OHTL parameters of Finote Selam

Table 4.13. Initial inputs and resistance of Finot Selam

Month	Uncertain parameters		Resistance change with temperature (Ω/m)	
	Wind speed (m/s)	Temperature ($^{\circ}C$)	RDC	RAC
Jan	[3.0400 3.9300]	[16.3881 18.0342]	[0.1039 0.1049]	[0.1554 0.1564]
Feb	[2.9600 3.9100]	[18.4468 20.2225]	[0.1030 0.1036]	[0.1542 0.1551]
Mar	[2.8900 3.7300]	[20.2713 21.7906]	[0.1021 0.1030]	[0.1533 0.1542]
Apr	[2.9100 3.7900]	[20.1643 22.4343]	[0.1018 0.1030]	[0.1530 0.1542]
May	[2.6100 3.3600]	[18.4439 19.8700]	[0.1030 0.1036]	[0.1545 0.1551]
Jun	[2.8600 3.3300]	[17.4263 18.8983]	[0.1036 0.1042]	[0.1548 0.1558]
Jul	[2.4900 2.8500]	[15.4823 17.2532]	[0.1042 0.1052]	[0.1558 0.1570]
Aug	[2.3000 2.6300]	[15.6565 16.6616]	[0.1045 0.1052]	[0.1564 0.1567]
Sep	[2.3800 2.5800]	[16.5050 17.1797]	[0.1042 0.1045]	[0.1561 0.1564]
Oct	[2.6400 3.4000]	[16.3597 17.1552]	[0.1042 0.1049]	[0.1561 0.1564]
Nov	[2.8800 3.1900]	[15.4300 16.5307]	[0.1045 0.1052]	[0.1564 0.1570]
Dec	[2.7900 3.6200]	[15.3590 18.3973]	[0.1039 0.1052]	[0.1551 0.1570]

Table 4.14. Sag and conductor length of Finote Selam

Month	Sag change (m)		Conductor length change (m)	
	DIA	DMC	LIA	LMC
Jan	[3.4735 4.0942]	[3.6690 3.8760]	[123.6033 123.7049]	[123.6330 123.6667]
Feb	[3.4564 4.0942]	[3.6570 3.8697]	[123.6008 123.7049]	[123.6312 123.6656]
Mar	[3.4859 3.9930]	[3.6472 3.8163]	[123.6052 123.6872]	[123.6296 123.6568]
Apr	[3.4756 4.0256]	[3.6499 3.8333]	[123.6036 123.6928]	[123.6300 123.6596]
May	[3.5055 3.8428]	[3.6144 3.7270]	[123.6081 123.6617]	[123.6245 123.6423]
Jun	[3.5674 3.7999]	[3.6432 3.7208]	[123.6176 123.6547]	[123.6290 123.6413]
Jul	[3.5649 3.6810]	[3.6031 3.6419]	[123.6172 123.6354]	[123.6227 123.6288]
Aug	[3.5605 3.6447]	[3.5883 3.6164]	[123.6166 123.6297]	[123.6204 123.6248]
Sep	[3.5770 3.6288]	[3.5942 3.6114]	[123.6191 123.6272]	[123.6213 123.6240]
Oct	[3.5035 3.8570]	[3.6175 3.7354]	[123.6078 123.6641]	[123.6249 123.6436]
Nov	[3.5983 3.7430]	[3.6458 3.6941]	[123.6224 123.6454]	[123.6294 123.6370]
Dec	[3.4881 3.9458]	[3.6344 3.7870]	[123.6055 123.6791]	[123.6276 123.6520]

Table 4.15. Resultant weight, tension, and resistance of Finote Selam

Month	Resultant weight change (kg/m)	Tension change (N)	Resistance change with the length of the conductor (Ω)	
	WRIA	HIA	RDC	RAC
Jan	[21.7441 22.9667]	[10102 9992]	[0.0138 0.0139]	0.0207 0.0208]
Feb	[21.6725 22.9294]	[10002 9885]	[0.0137 0.0138]	[0.0205 0.0207]
Mar	[21.6147 22.6147]	[9887 9793]	[0.0136 0.0137]	[0.0204 0.0205]
Apr	[21.6304 22.7147]	[9876 9800]	[0.0136 0.0137]	[0.0204 0.0205]
May	[21.4206 22.0853]	[9887 9844]	[0.0137 0.0138]	[0.0205 0.0207]
Jun	[21.5912 22.0500]	[9925 9919]	[0.0138 0.0139]	[0.0206 0.0207]
Jul	[21.3539 21.5833]	[9974 9927]	[0.0139 0.0140]	[0.0207 0.0209]
Aug	[21.2667 21.4324]	[9952 9930]	[0.0139 0.0140]	[0.0208 0.0209]
Sep	[21.3010 21.4039]	[9916 9901]	[0.0139 0.0139]	[0.0207 0.0208]
Oct	[21.4382 22.1363]	[10018 9945]	[0.0139 0.0139]	[0.0207 0.0208]
Nov	[21.6069 21.8912]	[10016 10009]	[0.0139 0.0140]	[0.0208 0.0209]
Dec	[21.5392 22.4422]	[10009 10008]	[0.0138 0.0140]	[0.0207 0.0209]

Worst-case Analysis of OHTL Parameters with Uncertainty using IA and MC approach

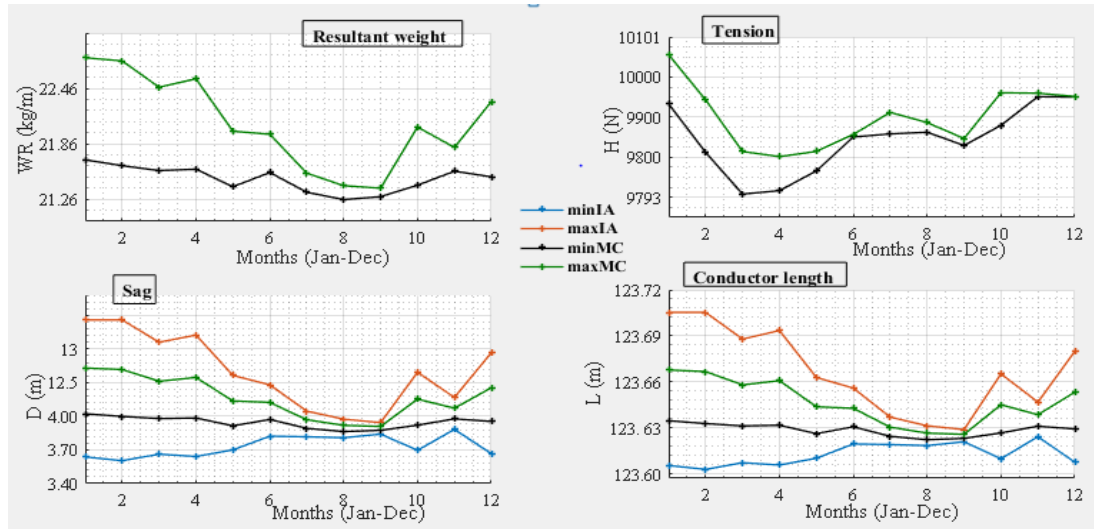


Figure 4.5. OHTL parameters variation for Finote Selam

4.1.6 OHTL parameters of Debre Markos city

Table 4.16. Initial inputs and resistance of Debre Markos

Month	Uncertain parameters		Resistance change with temperature (Ω/m)	
	Wind speed (m/s)	Temperature ($^{\circ}C$)	RDC	RAC
Jan	[2.1500 2.7100]	[17.6484 19.5823]	[0.1033 0.1042]	[0.1545 0.1558]
Feb	[2.1900 2.6600]	[20.2089 21.6972]	[0.1021 0.1030]	[0.1533 0.1542]
Mar	[2.2800 2.7700]	[21.9197 23.5103]	[0.1015 0.1021]	[0.1524 0.1533]
Apr	[2.0100 2.9200]	[21.3387 23.5503]	[0.1015 0.1024]	[0.1524 0.1536]
May	[1.8000 2.3000]	[20.0503 21.5274]	[0.1024 0.1030]	[0.1536 0.1542]
Jun	[1.8000 2.2600]	[19.1670 20.9277]	[0.1027 0.1033]	[0.1539 0.1548]
Jul	[1.7700 2.4800]	[16.5374 18.7213]	[0.1036 0.1045]	[0.1551 0.1564]
Aug	[1.8600 2.1400]	[16.7181 17.7719]	[0.1039 0.1045]	[0.1558 0.1561]
Sep	[1.7600 1.8500]	[17.6763 18.5193]	[0.1036 0.1042]	[0.1551 0.1558]
Oct	[2.3600 2.8800]	[17.0819 18.8923]	[0.1036 0.1045]	[0.1548 0.1561]
Nov	[2.3300 2.8500]	[16.7170 18.4970]	[0.1036 0.1045]	[0.1551 0.1561]
Dec	[2.1200 3.3300]	[16.4384 23.5]	[0.1015 0.1049]	[0.1524 0.1564]

Table 4.17. Sag and conductor length of Debre Markos

Month	Sag change (m)		Conductor length change (m)	
	DIA	DMC	LIA	LMC
Jan	[3.5335 3.6716]	[3.5789 3.6250]	[123.6124 123.6339]	[123.6190 123.6261]
Feb	[3.5434 3.6582]	[3.5812 3.6195]	[123.6139 123.6318]	[123.6193 123.6253]
Mar	[3.5426 3.6774]	[3.5870 3.6319]	[123.6138 123.6348]	[123.6202 123.6272]
Apr	[3.4940 3.7325]	[3.5717 3.6513]	[123.6064 123.6437]	[123.6179 123.6302]
May	[3.5387 3.6134]	[3.5634 3.5883]	[123.6132 123.6248]	[123.6166 123.6204]
Jun	[3.5413 3.6080]	[3.5634 3.5856]	[123.6136 123.6239]	[123.6166 123.6200]
Jul	[3.5231 3.6425]	[3.5624 3.6023]	[123.6108 123.6293]	[123.6164 123.6226]
Aug	[3.5527 3.5912]	[3.5655 3.5783]	[123.6154 123.6213]	[123.6169 123.6189]
Sep	[3.5591 3.5682]	[3.5621 3.5651]	[123.6163 123.6177]	[123.6164 123.6168]
Oct	[3.5403 3.6997]	[3.5926 3.6458]	[123.6134 123.6384]	[123.6211 123.6294]
Nov	[3.5398 3.6940]	[3.5904 3.6419]	[123.6134 123.6375]	[123.6207 123.6288]
Dec	[3.4395 3.8698]	[3.5772 3.7208]	[123.5982 123.6662]	[123.6187 123.6413]

Table 4.18. Resultant weight, tension, and resistance of Debre Markos

Month	Resultant weight change (kg/m)	Tension change (N)	Resistance change with the length of the conductor (Ω)	
	WRIA	HIA	RDC	RAC
Jan	[21.2108 21.4833]	[9846.5 9802.5]	[0.0137 0.0139]	[0.0206 0.0207]
Feb	[21.2245 21.4510]	[9730.0 9701.5]	[0.0136 0.0137]	[0.0204 0.0205]
Mar	[21.2588 21.5245]	[9658.4 9634.8]	[0.0135 0.0136]	[0.0203 0.0204]
Apr	[21.1686 21.6392]	[9669.1 9653.0]	[0.0135 0.0136]	[0.0203 0.0204]
May	[21.1186 21.2667]	[9718.9 9677.5]	[0.0136 0.0137]	[0.0204 0.0205]
Jun	[21.1186 21.2510]	[9759.8 9701.5]	[0.0137 0.0138]	[0.0205 0.0206]
Jul	[21.1137 21.3490]	[9883.5 9819.4]	[0.0138 0.0139]	[0.0206 0.0208]
Aug	[21.1314 21.2069]	[9878.1 9840.3]	[0.0138 0.0139]	[0.0207 0.0208]
Sep	[21.1108 21.1294]	[9828.7 9791.8]	[0.0138 0.0139]	[0.0206 0.0207]
Oct	[21.2922 21.6069]	[9887.0 9854.1]	[0.0138 0.0139]	[0.0206 0.0208]
Nov	[21.2784 21.5833]	[9902.6 9868.8]	[0.0138 0.0139]	[0.0206 0.0208]
Dec	[21.2010 22.0500]	[9903.0 9722.4]	[0.0135 0.0139]	[0.0203 0.0208]

Worst-case Analysis of OHTL Parameters with Uncertainty using IA and MC approach

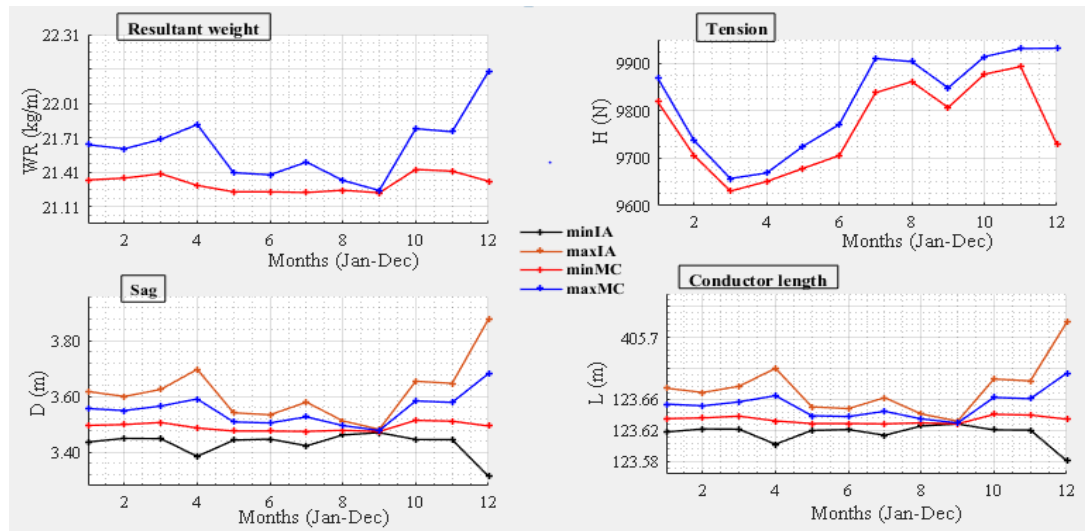


Figure 4.6. OHTL parameters variation for Debre Markos

4.1.7 OHTL parameters of Dejen city

Table 4.19. Initial inputs and resistance of Dejen

Month	Uncertain parameters		Resistance change with temperature (Ω/m)	
	Wind speed (m/s)	Temperature ($^{\circ}C$)	RDC	RAC
Jan	[1.8700 2.5500]	[17.3935 20.1590]	[0.1030 0.1042]	[0.1542 0.1558]
Feb	[2.1500 2.5700]	[19.8143 21.4900]	[0.1024 0.1030]	[0.1536 0.1545]
Mar	[2.0300 3.0300]	[21.2910 22.9100]	[0.1018 0.1024]	[0.1527 0.1536]
Apr	[1.8300 3.5300]	[20.8000 22.6233]	[0.1018 0.1027]	[0.1530 0.1539]
May	[1.9200 2.6000]	[20.1116 21.6223]	[0.1024 0.1030]	[0.1533 0.1542]
Jun	[1.8700 2.2200]	[19.9020 21.6290]	[0.1024 0.1030]	[0.1533 0.1545]
Jul	[1.6000 2.2300]	[16.5542 19.1684]	[0.1033 0.1045]	[0.1548 0.1564]
Aug	[1.5100 1.8000]	[16.6903 17.8703]	[0.1039 0.1045]	[0.1554 0.1564]
Sep	[1.6900 1.8000]	[17.5447 18.4840]	[0.1036 0.1042]	[0.1551 0.1558]
Oct	[2.3000 3.1800]	[16.7106 18.8452]	[0.1036 0.1045]	[0.1551 0.1561]
Nov	[2.3300 2.8700]	[16.5883 18.5667]	[0.1036 0.1045]	[0.1551 0.1564]
Dec	[1.8500 3.1000]	[16.4771 22.6233]	[0.1018 0.1045]	[0.1530 0.1564]

Table 4.20. Sag and conductor length of Dejen

Month	Sag change (m)		Conductor length change (m)	
	DIA	DMC	LIA	LMC
Jan	[3.5237 3.6517]	[3.5659 3.6086]	[123.6109 123.6308]	[123.6170 123.6236]
Feb	[3.5477 3.6423]	[3.5789 3.6105]	[123.6146 123.6293]	[123.6190 123.6238]
Mar	[3.4805 3.7645]	[3.5727 3.6674]	[123.6044 123.6489]	[123.6180 123.6328]
Apr	[3.3751 3.9760]	[3.5644 3.7648]	[123.5888 123.6843]	[123.6167 123.6484]
May	[3.5229 3.6595]	[3.5678 3.6134]	[123.6108 123.6320]	[123.6173 123.6243]
Jun	[3.5488 3.6003]	[3.5659 3.5831]	[123.6148 123.6227]	[123.6170 123.6196]
Jul	[3.5320 3.6098]	[3.5578 3.5837]	[123.6122 123.6242]	[123.6157 123.6197]
Aug	[3.5483 3.5710]	[3.5558 3.5634]	[123.6147 123.6182]	[123.6154 123.6166]
Sep	[3.5567 3.5667]	[3.5600 3.5634]	[123.6160 123.6175]	[123.6161 123.6166]
Oct	[3.4874 3.7991]	[3.5883 3.6923]	[123.6054 123.6545]	[123.6204 123.6367]
Nov	[3.5373 3.6993]	[3.5904 3.6445]	[123.6130 123.6384]	[123.6207 123.6292]
Dec	[3.4554 3.7955]	[3.5651 3.6786]	[123.6006 123.6539]	[123.6168 123.6346]

Table 4.21. Resultant weight, tension, and resistance of Dejen

Month	Resultant weight change (kg/m)	Tension change (N)	Resistance change with the length of the conductor (Ω)	
	WRIA	HIA	RDC	RAC
Jan	[21.1333 21.3863]	[9846.1 9759.8]	[0.0137 0.0139]	[0.0205 0.0207]
Feb	[21.2108 21.3971]	[9745.6 9702.0]	[0.0136 0.0137]	[0.0204 0.0206]
Mar	[21.1735 21.7343]	[9696.6 9672.2]	[0.0135 0.0136]	[0.0203 0.0204]
Apr	[21.1255 22.3098]	[9803.8 9686.0]	[0.0135 0.0137]	[0.0203 0.0205]
May	[21.1461 21.4137]	[9720.7 9698.9]	[0.0136 0.0137]	[0.0204 0.0205]
Jun	[21.1333 21.2343]	[9728.2 9667.7]	[0.0136 0.0137]	[0.0204 0.0205]
Jul	[21.0863 21.2382]	[9878.1 9780.3]	[0.0138 0.0139]	[0.0206 0.0208]
Aug	[21.0735 21.1186]	[9869.7 9820.7]	[0.0138 0.0139]	[0.0207 0.0208]
Sep	[21.0990 21.1186]	[9832.7 9791.8]	[0.0138 0.0139]	[0.0207 0.0207]
Oct	[21.2667 21.8804]	[9900.8 9900.8]	[0.0138 0.0139]	[0.0206 0.0208]
Nov	[21.2784 21.5990]	[9908.4 9867.9]	[0.0138 0.0139]	[0.0206 0.0208]
Dec	[21.1294 21.8000]	[9889.2 9720.2]	[0.0135 0.0139]	[0.0203 0.0208]

Worst-case Analysis of OHTL Parameters with Uncertainty using IA and MC approach

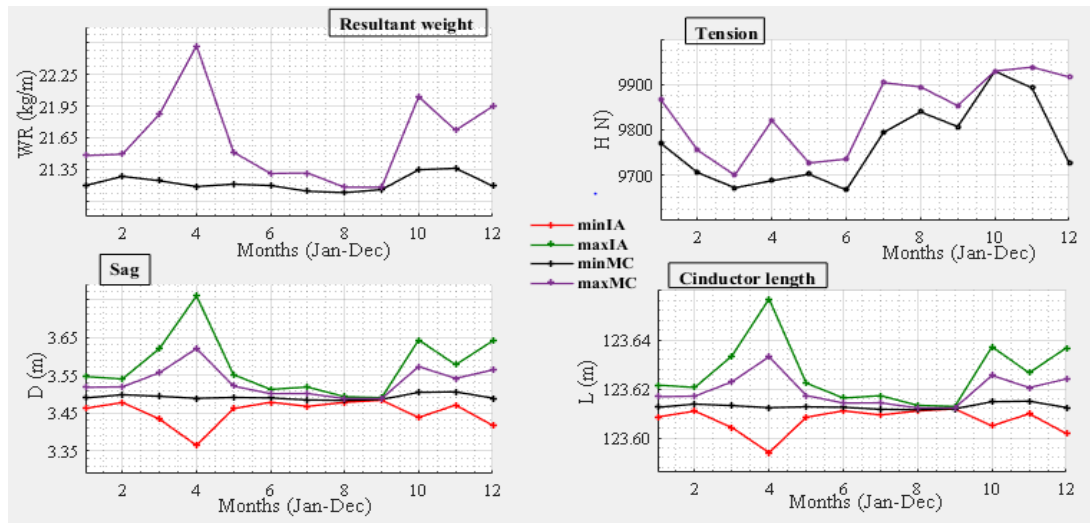


Figure 4.7. OHTL parameters variation for Dejen

4.1.8 OHTL parameters of Gerbe Gurach city

Table 4.22. Initial inputs and resistance of Gerbe Guaracha

Month	Uncertain parameters		Resistance change with temperature (Ω/m)	
	Wind speed (m/s)	Temperature ($^{\circ}C$)	RDC	RAC
Jan	[1.8600 2.9000]	[17.2087 20.4152]	[0.1027 0.1042]	[0.1542 0.1561]
Feb	[2.2700 2.8600]	[19.9554 21.6097]	[0.1024 0.1030]	[0.1533 0.1542]
Mar	[2.2300 3.2500]	[21.1994 22.9174]	[0.1018 0.1024]	[0.1527 0.1536]
Apr	[1.9000 3.6300]	[20.9340 22.7937]	[0.1018 0.1027]	[0.1527 0.1539]
May	[1.7400 2.5000]	[20.0155 21.4048]	[0.1024 0.1030]	[0.1536 0.1542]
Jun	[1.7800 2.1900]	[19.2810 21.1907]	[0.1024 0.1033]	[0.1536 0.1548]
Jul	[1.5400 2.2300]	[16.3048 18.8232]	[0.1036 0.1049]	[0.1551 0.1564]
Aug	[1.6400 1.8400]	[16.5294 17.7155]	[0.1042 0.1045]	[0.1558 0.1564]
Sep	[1.7400 1.8300]	[17.4297 18.3857]	[0.1039 0.1042]	[0.1551 0.1558]
Oct	[2.4900 3.1200]	[16.6271 19.0239]	[0.1036 0.1045]	[0.1548 0.1564]
Nov	[2.6000 2.8900]	[16.4580 18.8803]	[0.1036 0.1049]	[0.1548 0.1564]
Dec	[2.1000 3.3300]	[16.4319 18.8716]	[0.1036 0.1049]	[0.1548 0.1564]

Table 4.23. Sag and conductor length of Gerbe Gurach

Month	Sag change (m)		Conductor length change (m)	
	DIA	DMC	LIA	LMC
Jan	[3.4845 3.7333]	[3.5655 3.6485]	[123.6050 123.6438]	[123.6169 123.6298]
Feb	[3.5304 3.7009]	[3.5863 3.6432]	[123.6120 123.6386]	[123.6201 123.6290]
Mar	[3.4665 3.8305]	[3.5837 3.7052]	[123.6023 123.6597]	[123.6197 123.6388]
Apr	[3.3580 4.0256]	[3.5671 3.7896]	[123.5863 123.6928]	[123.6171 123.6524]
May	[3.5195 3.6470]	[3.5615 3.6040]	[123.6103 123.6300]	[123.6163 123.6229]
Jun	[3.5444 3.5998]	[3.5627 3.5812]	[123.6141 123.6227]	[123.6165 123.6193]
Jul	[3.5294 3.6111]	[3.5564 3.5837]	[123.6118 123.6244]	[123.6155 123.6197]
Aug	[3.5527 3.5708]	[3.5587 3.5648]	[123.6154 123.6181]	[123.6159 123.6168]
Sep	[3.5586 3.5674]	[3.5615 3.5644]	[123.6163 123.6176]	[123.6163 123.6167]
Oct	[3.5262 3.7623]	[3.6031 3.6820]	[123.6113 123.6485]	[123.6227 123.6351]
Nov	[3.5800 3.6812]	[3.6134 3.6472]	[123.6196 123.6355]	[123.6243 123.6296]
Dec	[3.4375 3.8710]	[3.5762 3.7208]	[123.5979 123.6665]	[123.6185 123.6413]

Table 4.24. Resultant weight, tension, and resistance of Gerbe Gurach

Month	Resultant weight change (kg/m)	Tension change (N)	Resistance change with the length of the conductor (Ω)	
	WRIA	HIA	RDC	RAC
Jan	[21.1314 21.6225]	[9854.5 9787.8]	[0.0137 0.0139]	[0.0205 0.0208]
Feb	[21.2549 21.5912]	[9746.5 9729.6]	[0.0136 0.0137]	[0.0204 0.0205]
Mar	[21.2382 21.9578]	[9734.0 9687.3]	[0.0135 0.0136]	[0.0203 0.0205]
Apr	[21.1402 22.4569]	[9820.3 9682.4]	[0.0135 0.0137]	[0.0203 0.0205]
May	[21.1069 21.3598]	[9718.9 9698.9]	[0.0136 0.0137]	[0.0204 0.0205]
Jun	[21.1147 21.2245]	[9754.0 9685.5]	[0.0136 0.0138]	[0.0204 0.0206]
Jul	[21.0775 21.2382]	[9889.2 9796.3]	[0.0138 0.0139]	[0.0206 0.0208]
Aug	[21.0912 21.1275]	[9880.3 9829.6]	[0.0139 0.0139]	[0.0207 0.0208]
Sep	[21.1069 21.1255]	[9839.9 9797.6]	[0.0138 0.0139]	[0.0207 0.0207]
Oct	[21.3539 21.8196]	[9919.0 9883.0]	[0.0138 0.0139]	[0.0206 0.0208]
Nov	[21.4137 21.6147]	[9936.8 9855.9]	[0.0138 0.0139]	[0.0206 0.0208]
Dec	[21.1951 22.0500]	[9926.2 9902.1]	[0.0138 0.0139]	[0.0206 0.0208]

Worst-case Analysis of OHTL Parameters with Uncertainty using IA and MC approach

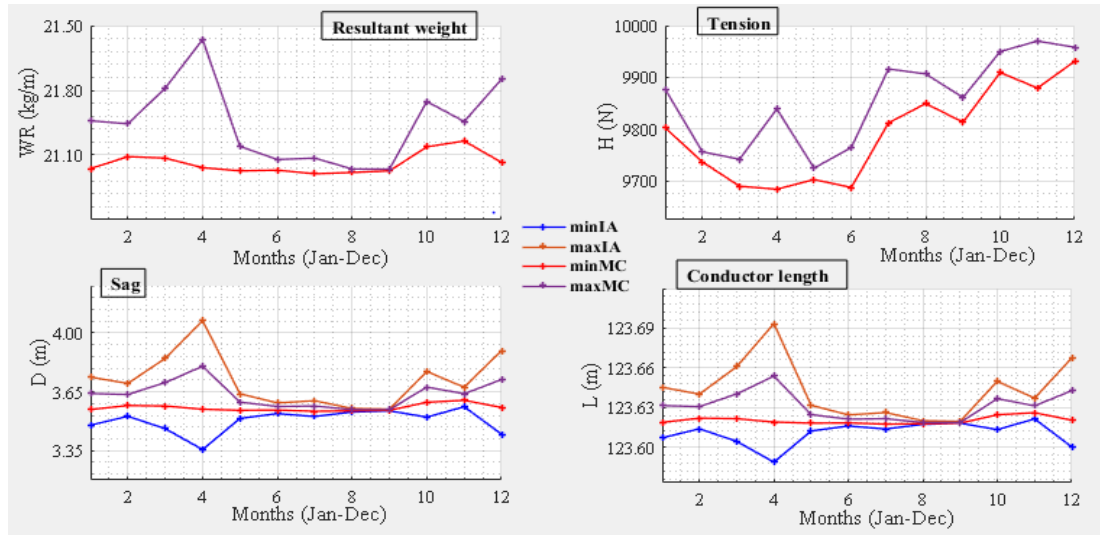


Figure 4.8. OHTL parameters variation for Gerbe Gurach

4.1.9 OHTL parameters of Ficha city

Table 4.25. Initial inputs and resistance of Ficha

Month	Uncertain parameters		Resistance change with temperature (Ω/m)	
	Wind speed (m/s)	Temperature ($^{\circ}C$)	RDC	RAC
Jan	[2.4800 3.7800]	[15.1100 18.5800]	[0.1036 0.1055]	[0.1551 0.1570]
Feb	[2.7400 3.8800]	[18.1300 19.3500]	[0.1033 0.1039]	[0.1548 0.1554]
Mar	[2.8600 4.2400]	[19.3200 20.8100]	[0.1027 0.1033]	[0.1539 0.1548]
Apr	[2.4300 4.5400]	[18.9300 20.5400]	[0.1027 0.1036]	[0.1539 0.1548]
May	[2.6600 3.4800]	[18.7300 20.0700]	[0.1030 0.1036]	[0.1542 0.1551]
Jun	[1.9100 2.9100]	[18.6700 20.3400]	[0.1030 0.1036]	[0.1542 0.1551]
Jul	[1.8900 2.4700]	[15.5500 18.2000]	[0.1039 0.1052]	[0.1554 0.1570]
Aug	[1.6800 2.1700]	[15.9000 17.0900]	[0.1045 0.1049]	[0.1561 0.1567]
Sep	[2.3400 2.5800]	[16.3700 17.4400]	[0.1042 0.1049]	[0.1558 0.1564]
Oct	[3.1900 4.2500]	[15.3600 17.2300]	[0.1042 0.1052]	[0.1561 0.1570]
Nov	[3.4200 3.9700]	[15.0300 16.8600]	[0.1045 0.1055]	[0.1561 0.1573]
Dec	[2.7900 4.1600]	[14.5500 16.9300]	[0.1045 0.1055]	[0.1561 0.1573]

Table 4.26. Sag and conductor length of Ficha

Month	Sag change (m)		Conductor length change (m)	
	DIA	DMC	LIA	LMC
Jan	[3.3881 4.0726]	[3.6023 3.8305]	[123.5907 123.7011]	[123.6226 123.6591]
Feb	[3.4110 4.1064]	[3.6284 3.8603]	[123.5940 123.7071]	[123.6266 123.6641]
Mar	[3.3307 4.3599]	[3.6432 3.9858]	[123.5823 123.7534]	[123.6290 123.6853]
Apr	[3.1480 4.7023]	[3.5981 4.1138]	[123.5567 123.8205]	[123.6219 123.7076]
May	[3.4910 3.8914]	[3.6196 3.7532]	[123.6059 123.6699]	[123.6253 123.6465]
Jun	[3.4870 3.7341]	[3.5674 3.6499]	[123.6053 123.6439]	[123.6172 123.6300]
Jul	[3.5322 3.6365]	[3.5666 3.6014]	[123.6122 123.6284]	[123.6171 123.6224]
Aug	[3.5397 3.6004]	[3.5598 3.5800]	[123.6134 123.6227]	[123.6160 123.6191]
Sep	[3.5710 3.6318]	[3.5912 3.6114]	[123.6182 123.6277]	[123.6209 123.6240]
Oct	[3.4211 4.3083]	[3.6942 3.9896]	[123.5955 123.7438]	[123.6370 123.6859]
Nov	[3.5966 4.0438]	[3.7398 3.8889]	[123.6221 123.6960]	[123.6443 123.6689]
Dec	[3.3400 4.3040]	[3.6344 3.9554]	[123.5837 123.7430]	[123.6276 123.6801]

Table 4.27. OHTL resultant weight, tension, and resistance of Ficha

Month	Resultant weight change (kg/m)	Tension change (N)	Resistance change with the length of the conductor (Ω)	
	WRIA	HIA	RDC	RAC
Jan	[21.3490 22.6980]	[10039 9992]	[0.0138 0.0140]	[0.0206 0.0209]
Feb	[21.5029 22.8735]	[10031 9872]	[0.0137 0.0138]	[0.0206 0.0207]
Mar	[21.5912 23.6167]	[10077 9832]	[0.0137 0.0138]	[0.0205 0.0206]
Apr	[21.3235 24.3735]	[10191 9806]	[0.0137 0.0138]	[0.0205 0.0207]
May	[21.4510 22.2412]	[9903 9836]	[0.0137 0.0138]	[0.0205 0.0206]
Jun	[21.1431 21.6304]	[9793 9787]	[0.0137 0.0138]	[0.0205 0.0206]
Jul	[21.1373 21.3441]	[9936 9843]	[0.0138 0.0140]	[0.0207 0.0209]
Aug	[21.0980 21.2176]	[9912 9875]	[0.0139 0.0140]	[0.0208 0.0208]
Sep	[21.2824 21.4039]	[9920 9888]	[0.0139 0.0139]	[0.0207 0.0208]
Oct	[21.8912 23.6392]	[10230 10064]	[0.0139 0.0140]	[0.0207 0.0209]
Nov	[22.1618 23.0441]	[10164 10121]	[0.0139 0.0140]	[0.0208 0.0209]
Dec	[21.5392 23.4363]	[10216 10048]	[0.0139 0.0141]	[0.0208 0.0210]

Worst-case Analysis of OHTL Parameters with Uncertainty using IA and MC approach

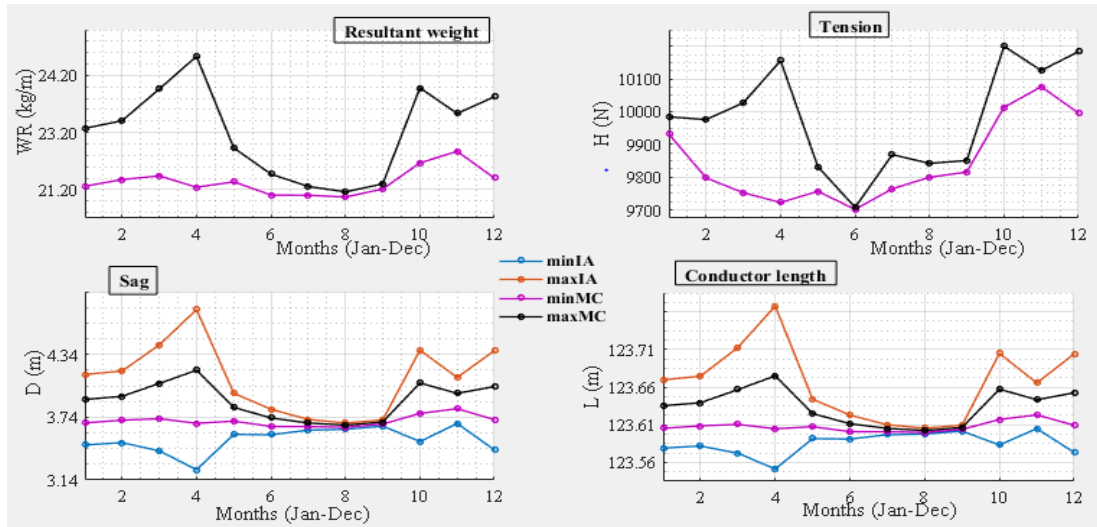


Figure 4.9. OHTL parameters variation for Fichta

4.1.10 OHTL parameters of Addis Ababa city

Table 4.28. Initial inputs and resistance of Addis Ababa

Month	Uncertain parameters		Resistance change with temperature (Ω/m)	
	Wind speed (m/s)	Temperature ($^{\circ}C$)	RDC	RAC
Jan	[3.1200 4.6300]	[13.2994 16.2323]	[0.1049 0.1061]	[0.1564 0.1582]
Feb	[2.9900 4.6900]	[4.2193 17.4355]	[0.1042 0.1103]	[0.1558 0.1634]
Mar	[3.1800 5.2800]	[17.1958 18.7735]	[0.1036 0.1042]	[0.1551 0.1561]
Apr	[2.6500 5.5100]	[16.9333 18.9283]	[0.1036 0.1045]	[0.1548 0.1561]
May	[3.1000 4.1800]	[16.7106 18.0555]	[0.1039 0.1045]	[0.1554 0.1561]
Jun	[2.2700 3.3000]	[16.8230 18.3060]	[0.1039 0.1045]	[0.1554 0.1561]
Jul	[2.3600 3.2500]	[14.5100 16.4877]	[0.1045 0.1058]	[0.1564 0.1576]
Aug	[2.0900 2.7200]	[14.6755 15.7190]	[0.1052 0.1055]	[0.1567 0.1573]
Sep	[2.8900 3.2600]	[14.7067 15.6710]	[0.1052 0.1055]	[0.1567 0.1573]
Oct	[4.0600 5.2800]	[13.6042 15.1410]	[0.1055 0.1061]	[0.1570 0.1579]
Nov	[4.3600 4.8100]	[13.1263 14.8150]	[0.1055 0.1064]	[0.1573 0.1582]
Dec	[3.2900 5.1100]	[12.7842 18.4948]	[0.1036 0.1064]	[0.1551 0.1585]

Table 4.29. Sag and conductor length of Addis Ababa

Month	Sag change (m)		Conductor length change (m)	
	DIA	DMC	LIA	LMC
Jan	[3.2624 4.6914]	[3.6821 4.1568]	[123.5726 123.8183]	[123.6351 123.7153]
Feb	[3.2032 4.7854]	[3.6614 4.1866]	[123.5643 123.8376]	[123.6318 123.7206]
Mar	[3.0111 5.5554]	[3.6924 4.5304]	[123.5385 124.0097]	[123.6367 123.7851]
Apr	[2.7935 6.0760]	[3.6186 4.6906]	[123.5112 124.1406]	[123.6251 123.8169]
May	[3.4154 4.2683]	[3.6786 3.9629]	[123.5947 123.7364]	[123.6346 123.6814]
Jun	[3.4625 3.8477]	[3.5863 3.7148]	[123.6017 123.6626]	[123.6201 123.6403]
Jul	[3.4838 3.8210]	[3.5926 3.7052]	[123.6049 123.6581]	[123.6211 123.6388]
Aug	[3.5260 3.6772]	[3.5757 3.6261]	[123.6113 123.6348]	[123.6185 123.6263]
Sep	[3.5884 3.7678]	[3.6472 3.7071]	[123.6209 123.6494]	[123.6296 123.6391]
Oct	[3.3924 5.2344]	[3.9195 4.5304]	[123.5913 123.9348]	[123.6740 123.7851]
Nov	[3.8315 4.4739]	[4.0345 4.2488]	[123.6599 123.7752]	[123.6937 123.7319]
Dec	[3.1193 5.2629]	[3.7129 4.4214]	[123.5529 123.9413]	[123.6400 123.7641]

Table 4.30. Resultant weight, tension, and resistance of Addis Ababa

Month	Resultant weight change (kg/m)	Tension change (N)	Resistance change with the length of the conductor (Ω)	
	WRIA	HIA	RDC	RAC
Jan	[21.8206 24.6265]	[10400 101530]	[0.0139 0.0142]	[0.0208 0.0211]
Feb	[21.6990 24.8020]	[10610 10370]	[0.0139 0.0147]	[0.0207 0.0218]
Mar	[21.8804 26.8314]	[10550 9980]	[0.0138 0.0139]	[0.0206 0.0208]
Apr	[21.4451 27.7765]	[10640 9920]	[0.0138 0.0140]	[0.0206 0.0209]
May	[21.8010 23.4804]	[10170 9990]	[0.0138 0.0139]	[0.0207 0.0208]
Jun	[21.2549 22.0137]	[9950 9890]	[0.0138 0.0139]	[0.0207 0.0208]
Jul	[21.2922 21.9569]	[10020 10010]	[0.0139 0.0141]	[0.0208 0.0210]
Aug	[21.1912 21.4902]	[9990 9980]	[0.0140 0.0140]	[0.0209 0.0209]
Sep	[21.6147 21.9686]	[10060 10050]	[0.0140 0.0140]	[0.0209 0.0209]
Oct	[23.2235 26.8314]	[10690 10340]	[0.0140 0.0141]	[0.0209 0.0211]
Nov	[23.9039 25.1696]	[10520 10440]	[0.0140 0.0142]	[0.0209 0.0211]
Dec	[22.0029 26.1882]	[10490 10210]	[0.0138 0.0142]	[0.0206 0.0211]

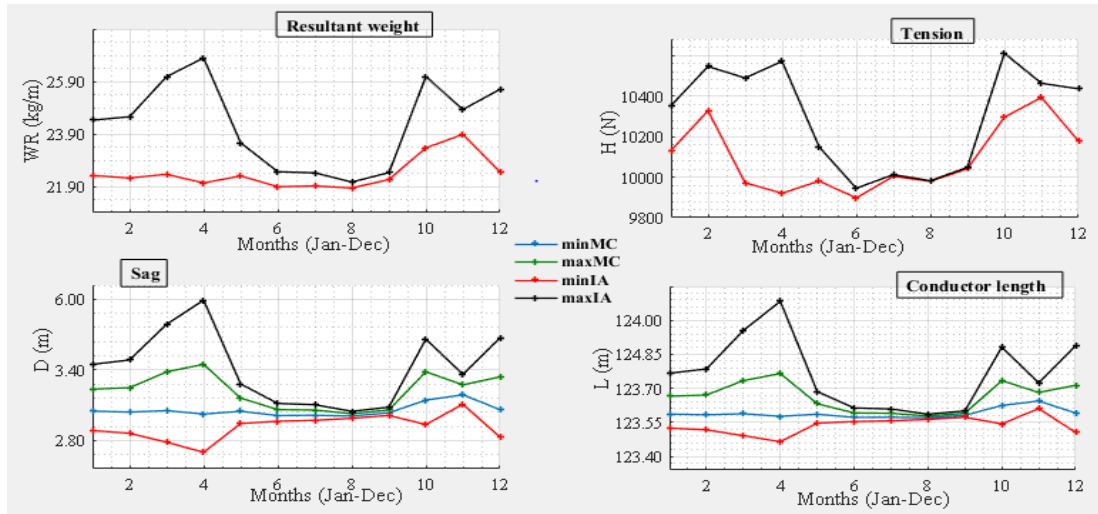


Figure 4.10. OHTL parameters variation for Addis Ababa

4.2 Discussion

In this thesis, All aluminum alloy conductor (AAAC) is used to verify the proposed methods. The constants, which are used in finding all the variables for AAAC's, are as follows: $A=0.0008507 m^2$, $l=123.9 m$, $W_b=21.0294 kg/m$, $\varepsilon =11.5*10^6 Mpsi$, $\alpha_T =23*10^{-6} / ^\circ C$, $H_o=12391 N$ $c=0$, $k=0$. The DC and AC resistance of the AAAC conductor at $20^\circ C$ and $75^\circ C$, are $0.10973 \Omega/m$ and $0.13167 \Omega/m$ respectively.

In this thesis, the initial tension and span length are chosen from the collected data from EPU northwest region Bahir dar district as shown in appendix B. It is clear that nothing is certain in the temperature and wind speed varying environment for OHTL, and thus adopting a model that considers such uncertainty is mandatory. The question to be answered is whether the proposed method is effective in considering uncertainty than the traditional mechanism or not. However, uncertainty is the change of OHTL parameters from lower to higher bounds. To validate the values of sag, tension, and conductor length of an overhead transmission line is conservative with an uncertain environment the MC and IA based computational methods are used and compared. The two methods are implemented using Mat lab software. For the MC method, 10,000 random variables for wind pressure and temperature are generated using Mat lab in between the defined bound

to get non-varying results. The long span catenary curve between two supports (towers) of the leveled span is used as a sample only to study the effect of OHTL parameters, sag, tension, and conductor length with the variation of temperature and wind speed.

In the Table, I, II, III (Appendix D) the variation in between the interval is from lower to higher or vice versa, depending on the combined effect of change of values.

Table I (Appendix D.1) shows the uncertain inputs and resistance change with the given temperature of 10 cities respectively. For the uncertain inputs, the lower bounds result corresponds to the lower input and the upper bound results correspond to the upper input for each month.

Table II (Appendix D.2) shows the sag and conductor length of the overhead transmission line of 10 cities respectively. For sag and conductor length, the lower bound corresponds to the minimum for each algorithm and it is due to the lower temperature and weight. Similarly, the upper bound corresponds to the maximum for each algorithm and it is due to the upper bound temperature and weight for each month. For decreasing temperature at each table the corresponding sag and conductor length increases. The increasing of wind pressure at each table results increasing in sag and conductor length. Also, decreasing sag results in the minimum conductor length, since conductor length and sag is related directly.

Table III (Appendix D.3) shows the resultant weight, tension, and resistance change with conductor length. For resultant weight, DC resistance and Ac resistance, the lower bound corresponds to the minimum value and the upper bound is the maximum for each month, and the tension is reversed. In all cities, the change in conductor length changes the overall AC and DC resistance in each span of the overhead transmission line. The tension value depends on the loading condition and the temperature changes. It decreases in value for some values changes in temperature even though the loading increases for the particular temperature change and is affected by the resultant weight of the cable. Since tension is inversely proportional to resultant weight and sag of OHTL.

The worst-case 10 cities of Resultant weight, tension, sag, and conductor length is depicted in Fig. 4.1-4.10. Since there is a little effect on the round of and truncation error in the calculation of the resultant weight and sag. The results due to the IA and MC approach is similar for four significant figures. However, when the manipulation and uncertainty inclusion increases, there will be differences in the result of the IA and MC approaches. Hence in all the OHTL parameters, the IA based approach provides the worst case result than the probabilistic MC approach.

For Bahir Dar city, the resultant conductor weight, in the worst-case scenario, varies from the minimum 21.6549 kg/m to 23.6049 kg/m, the tension changes from 10031.6 N to 9790.5 N, the sag and conductor length changes from the minimum 3.4363 m and 123.5978 m to 4.2893 m and 123.7402 m, respectively.

For Dangila city, the resultant conductor weight, in the worst-case scenario, varies from the minimum 21.5608 kg/m to 24.3451 kg/m, the tension changes from 10131.6 N to 9796.7 N, the sag and conductor length changes from the minimum 3.4880 m and 123.6055 m to 4.3525 m and 123.7520 m, respectively.

For Enjibara city, the resultant conductor weight, in the worst-case scenario, varies from the minimum 21.3804 kg/m to 23.9529 kg/m, the tension changes from 10088.06 N to 9747.35 N, the sag and conductor length changes from the minimum 3.3966 m and 123.5919 m to 4.3210 m and 123.7461 m, respectively.

For Bura city, the resultant conductor weight, in the worst-case scenario, varies from the minimum 21.0814 kg/m to 21.4765 kg/m, the tension changes from 9950.62 N to 9671.73 N, the sag and conductor length changes from the minimum 3.5195 m and 123.6103 m to 3.6772 m and 123.6348 m, respectively.

For Finot Selam city, the resultant conductor weight, in the worst-case scenario, varies from the minimum 21.2667 kg/m to 22.9667 kg/m, the tension changes from 10101.85 N to 9793.16 N, the sag and conductor length changes from the minimum 3.4564 m and 123.6008 m to 4.0942 m and 123.7049 m, respectively.

Worst-case Analysis of OHTL Parameters with Uncertainty using IA and MC approach

For Debre Markos city, the resultant conductor weight, in the worst-case scenario, varies from the minimum 21.1109 kg/m to 22.05 kg/m, the tension changes from 9903.03 N to 9634.81 N, the sag and conductor length changes from the minimum 3.4395 m and 123.5982 m to 3.8698 m and 123.6662 m, respectively.

For Dejen city, the resultant conductor weight, in the worst-case scenario, varies from the minimum 21.0735 kg/m to 22.3167 kg/m, the tension changes from 9908.36 N to 9667.73 N, the sag and conductor length changes from the minimum 3.3757 m and 123.5887 m to 3.9760 m and 123.6842 m, respectively.

For Gerb Gurach city, the resultant conductor weight, in the worst-case scenario, varies from the minimum 21.0774 kg/m to 22.45 kg/m, the tension changes from 9936.83 N to 9682.41 N, the sag and conductor length changes from the minimum 3.3580 m and 123.5862 m to 4.0256 m and 123.6928 m, respectively.

For Ficha city, the resultant conductor weight, in the worst-case scenario, varies from the minimum 21.0980 kg/m to 24.3716 kg/m, the tension changes from 10229.95 N to 9786.93 N, the sag and conductor length changes from the minimum 3.1479 m and 123.5567 m to 4.7023 m and 123.8205 m, respectively.

For Addis Ababa city, the resultant conductor weight, in the worst-case scenario, varies from the minimum 21.1912 kg/m to 27.7765 kg/m, the tension changes from 10685.87 N to 9893.24 N, the sag and conductor length changes from the minimum 2.7935 m and 123.5112 m to 6.0759 m and 124.1431 m, respectively.

Therefore, from 10 cities the worst-case scenario values of OHTL parameters is recorded in Addis Ababa city with the uncertain results by IA approach of resultant conductor weight is 6.5853 kg/m, tension is 792.63 N, sag is 3.2824 m, and conductor length is 0.6319 m and MC results of resultant conductor weight are 6.5853 kg/m, tension is 792.63 N, sag is 1.0720 m, and conductor length is 0.1917 m is recorded the minimum in February and the maximum in April respectively (except for tension is reversed).

Worst-case Analysis of OHTL Parameters with Uncertainty using IA and MC approach

The small change of OHTL parameters is also observed in Bura city with the uncertain values by IA approach of resultant conductor weight is 0.3951 kg/m, tension is 278.89 N, sag is 0.1577 m and conductor length is 0.0245 m. and MC results of resultant conductor weight is 0.3951 kg/m, tension is 278.89 m, sag is 0.0526 m, and conductor length is 0.0082 m is recorded in February.

In the worst-case, the temperature changes from 4.2193 °C to 18.9283 °C and the wind speed 2.0900 m/s to 5.5100 m/s has recorded the minimum in February and the maximum in April respectively for both temperature and wind, the corresponding tension change by IA approach is 792.63 N which is a very large value.

Also, in 400kV OHTL installed data of one section, the value of tension change for the temperature of 5 °C to 20 °C is 2153 N is calculated by the ordinary single point method which is also a very large value compared to the IA approach.

Therefore, as we see in the above description of the changes of overhead transmission line parameters, the change of temperature and wind speed in the worst-case highly affects OHTL by varying the values of its parameters from lower to upper extremes. To overcome such a problem, the change analysis methods IA is a very important approach to get conservative results rather than MC.

Chapter 5

Conclusion and recommendations

5.1 Conclusion

The effect of temperature change and wind pressure loading on OHTL parameters sag, tension, conductor length, and resistances have been presented in this paper. Sag and tension calculation using the Catenary method ignores small errors besides the error created during manipulation. Such an error added to the uncertainty in the main variables creates the final results inaccurate. The proposed IA based approach is validated using the MC approach as a conservative algorithm than probabilistic. In terms of time consumption, IA simulation is effective than the probabilistic MC approach which takes 10,000 iterations to converge. Based on the tabulated and graphed results, the IA approach is slightly conservative than MC approaches. This is mainly due to its ability to consider all sorts of uncertainty and tracks the relationship between variables than MC approaches.

The variability of the results for 10 cities of OHTL parameters shows that the ordinary single point approach fails to give worst-case results of OHTL parameters in a single calculation. Eventually, IA based calculation gives the worst case result of sag, tension, and conductor length of the transmission line for the experts to take action for reliable power delivery. The proposed algorithm can be extended to study the capacitance and inductance of OTL with temperature variation.

5.2 Recommendation

The Overhead transmission line is a very necessary resource to perform day to day activities. To deliver reliable electric power to the load, the OHTL parameters sag, tension and conductor length should be maintained with their optimum value. This thesis recommended that the experts should calculate the overhead transmission line parameters by computational algorithms, especially by IA approach rather than ordinary single point at the time of installing new transmission line Science, Ethiopian electric power operators

switch of mostly the distribution systems at the time of rain and windy day. Therefore, calculating overhead transmission line resultant weight, sag, tension, conductor length and resistance (DC&AC) by computational methods specially by IA are important to overcome the above problems.

Reference

- [1] M. Z. Abbasi, M. A. Aman, H. U. Afridi, and A. Khan, “Sag-Tension Analysis of AAAC Overhead Transmission lines for Hilly Areas,” no. December, 2018.
- [2] F. Oluwajobi, O. Ale, and A. Ariyanninuola, “Effect of Sag on Transmission Line,” *J. Emerg. Trends Eng. Appl. Sci.*, vol. 3, no. 4, pp. 627–630, 2012.
- [3] S. Malhara and V. Vittal, “Monitoring sag and tension of a tilted transmission line using geometric transformation,” *2009 IEEE Power Energy Soc. Gen. Meet. PES '09*, pp. 1–7, 2009, doi: 10.1109/PES.2009.5275935.
- [4] A. Hatibovic and P. Kadar, “An algorithm for the parabolic approximation of the catenary applicable in both inclined and level spans,” *CANDO-EPE 2018 - Proc. IEEE Int. Conf. Work. Obuda Electr. Power Eng.*, pp. 217–221, 2019, doi: 10.1109/CANDO-EPE.2018.8601137.
- [5] J. Jiang, Z. Jia, X. Wang, S. Wang, and C. Yang, “Analysis of conductor sag change after bare overhead conductor is covered with insulation material,” *ICEMPE 2019 - 2nd Int. Conf. Electr. Mater. Power Equipment, Proc.*, pp. 439–442, 2019, doi: 10.1109/ICEMPE.2019.8727396.
- [6] A. Molaei, “Extracting of Sagging Profile of Overhead Power

Transmission Line Via Image Processing,” *2018 IEEE Can. Conf. Electr. Comput. Eng.*, pp. 1–5, 2018.

- [7] S. Islam and F. Islam, “Impact of Temperature, Wind Flow, Solar Radiation, Skin Effect and Proximity Effect on Overhead Conductor,” *Glob. J. Res. Eng. Electr. Electron. Eng.*, vol. 12, no. 1, p. 5, 2012.
- [8] B. Sun, L. Hou, G. Fu, X. Meng, Z. Guan, and L. Wang, “Study of dynamic response of overhead transmission lines to different wind speeds,” *2010 Int. Conf. High Volt. Eng. Appl. ICHVE 2010*, no. 4, pp. 622–625, 2010, doi: 10.1109/ICHVE.2010.5640780.
- [9] Y. M. Abebe, “Overhead Transmission Line Sag , Tension and Length Calculation using Affine Arithmetic,” 2015.
- [10] I. Hathout and D. Ph, “Impact of Thermal Stresses on the End of Life of Overhead Transmission Conductors,” *2018 IEEE Power Energy Soc. Gen. Meet.*, pp. 1–5, 2018.
- [11] B. Liu, “Why is there a need for uncertainty theory?,” *J. Uncertain Syst.*, vol. 6, no. 1, pp. 3–10, 2012, doi: 10.1002/eqe.1037.
- [12] T. S. Hlalele and S. Du, “Analysis of Power Transmission Line Uncertainties: Status Review,” *J. Electr. Electron. Syst.*, vol. 5, no. 3, 2016, doi: 10.4172/2332-0796.1000194.
- [13] Y. Mekonnen Abebea, P. M. Rao, and M. G. Naik, “Analysis of Overhead Transmission Line Parameters with Uncertainty,” *Int. J. Eng. Manuf.*, vol. 7, no. 5, pp. 16–30, 2017, doi: 10.5815/ijem.2017.05.02.

- [14] M. Asprou, E. Kyriakides, S. Member, M. M. Albu, and S. Member, “Uncertainty Bounds of Transmission Line Parameters Estimated From Synchronized Measurements,” *IEEE Trans. Instrum. Meas.*, vol. PP, pp. 1–11, 2020, doi: 10.1109/TIM.2018.2867966.
- [15] Y. Unis Hijazi, H. Hagen, C. Hansen, and K. I. Joy, “Why interval arithmetic is so useful,” pp. 148–163.
- [16] T. Hickey, Q. Ju, and M. H. Van Emden, “Interval arithmetic: From principles to implementation,” *J. ACM*, vol. 48, no. 5, pp. 1038–1068, 2001, doi: 10.1145/502102.502106.
- [17] J. C. Araujo and S. Bedoui, “Lightning performance analysis of transmission lines using the Monte Carlo method and parallel computing Análisis del comportamiento de líneas de transmisión frente al rayo mediante el método de Monte Carlo y cálculo paralelo,” vol. 26, pp. 398–409, 2018.
- [18] M. Schl, S. Member, and P. Mancarella, “Probabilistic Modeling and Simulation of Transmission Line Temperatures under Fluctuating Power Flows,” pp. 1–9.
- [19] M. Keshavarzian and C. H. Priebe, “Sag and tension calculations for overhead transmission lines at high temperatures - modified ruling span method,” *IEEE Trans. Power Deliv.*, vol. 15, no. 2, pp. 777–783, 2000, doi: 10.1109/61.853019.
- [20] K. Adomah, Y. Mizuno, and K. Naito, “Probabilistic assessment of the reduction in tensile strength of an overhead transmission line’s

- conductor with reference to climatic data,” *IEEE Power Eng. Rev.*, vol. 20, no. 5, p. 80, 2000, doi: 10.1109/tdcllm.1998.668348.
- [21] R. G. Olsen and K. S. Edwards, “A New Method for Real-Time Monitoring of High-Voltage Transmission Line Conductor Sag,” *IEEE Power Eng. Rev.*, vol. 22, no. 6, pp. 62–63, 2002, doi: 10.1109/MPER.2002.4312315.
- [22] A. Piccolo, A. Vaccaro, D. Villacci, and M. Ieee, “An Affine Arithmetic based methodology for the thermal rating assessment of Overhead Lines in the presence of Data Uncertainty,” 2003.
- [23] H. Shaalan, “Calculating transmission line inductance using interval mathematics,” *2004 Int. Conf. Probabilistic Methods Appl. to Power Syst.*, pp. 224–226, 2004.
- [24] S. Kurokawa, J. P. Filho, M. C. Tavares, C. M. Portela, L. S. Member, and A. J. Prado, “Behavior of Overhead Transmission Line Parameters on the Presence of Ground Wires,” vol. 20, no. 2, pp. 1669–1676, 2005.
- [25] A. F. Abdel-Gawad and A. S. A. Zoklot, “Wind and environmental effects on overhead high voltage transmission lines,” *WIT Trans. Ecol. Environ.*, vol. 93, pp. 433–443, 2006, doi: 10.2495/SC060411.
- [26] P. Ramachandran, V. Vittal, and G. T. Heydt, “Mechanical state estimation for overhead transmission lines with level spans,” *IEEE Trans. Power Syst.*, vol. 23, no. 3, pp. 908–915, 2008, doi: 10.1109/TPWRS.2008.926093.

- [27] M. Muhr, S. Pack, and S. Jaufer, “Usage and benefit of an overhead line monitoring system,” *2008 Int. Conf. High Volt. Eng. Appl. ICHVE 2008*, pp. 557–561, 2008, doi: 10.1109/ICHVE.2008.4773996.
- [28] H. Shaalan and K. Point, “TRANSMISSION LINE ANALYSIS USING,” pp. 0–4, 2012.
- [29] S. Q. Chen, J. M. Li, T. Luo, H. Y. Zhou, Q. X. Ma, and L. Du, “Performance of overvoltage transducer for overhead transmission lines,” *2013 IEEE Int. Conf. Appl. Supercond. Electromagn. Devices, ASEMD 2013*, pp. 48–51, 2013, doi: 10.1109/ASEMD.2013.6780705.
- [30] A. Polevoy, “Impact of Data Errors on Sag Calculation Accuracy for Overhead Transmission Line,” vol. 29, no. 5, pp. 2040–2045, 2014.
- [31] G. Sivanagaraju, S. Chakrabarti, and S. C. Srivastava, “Uncertainty in transmission line parameters: Estimation and impact on line current differential protection,” *IEEE Trans. Instrum. Meas.*, vol. 63, no. 6, pp. 1496–1504, 2014, doi: 10.1109/TIM.2013.2292276.
- [32] A. Hatibovic, “Derivation of equations for conductor and sag curves of an overhead line based on a given catenary constant,” *Period. Polytech. Electr. Eng. Comput. Sci.*, vol. 58, no. 1, pp. 23–27, 2014, doi: 10.3311/PPee.6993.
- [33] R. Yao, K. Sun, F. Liu, and S. Mei, “Efficient simulation of temperature evolution of overhead transmission lines based on analytical solution and NWP,” *IEEE Trans. Power Deliv.*, vol. 33, no. 4, pp. 1576–1588, 2018, doi: 10.1109/TPWRD.2017.2751563.

- [34] D. Sacerdotianu, M. Nicola, C. I. Nicola, and F. Lazarescu, “Research on the continuous monitoring of the sag of overhead electricity transmission cables based on the measurement of their slope,” *2018 Int. Conf. Appl. Theor. Electr. ICATE 2018 - Proc.*, pp. 0–4, 2018, doi: 10.1109/ICATE.2018.8551427.
- [35] et al. Noor, “Temperature and wind impacts on sag and tension of AAAC overhead transmission line,” *Int. J. Adv. Appl. Sci.*, vol. 5, no. 2, pp. 14–18, 2018, doi: 10.21833/ijaas.2018.02.003.
- [36] “Underground vs . Overhead Transmission and Distribution,” pp. 1–21, 2009.
- [37] I. Albizu, E. Fernández, A. J. Mazón, M. Bediauneta, and K. Sagastabeitia, “Overhead conductor monitoring system for the evaluation of the low sag behavior,” pp. 1–6, 2011.
- [38] M. Tenzer, H. Koch, and D. Imamovic, “Underground transmission lines for high power AC and DC transmission,” *Proc. IEEE Power Eng. Soc. Transm. Distrib. Conf.*, vol. 2016-July, 2016, doi: 10.1109/TDC.2016.7519942.
- [39] P. Kerdpradu, “Comparative study for the installation of overhead ground wire affecting the electric field of high voltage transmission lines,” no. x, pp. 1–7, 2014.
- [40] J. Bradbury and G. F. Kuska, “Sag and tension calculations for mountainous terrain,” vol. 130, no. 4, pp. 1982–1983, 1983.
- [41] C. Curve and R. Deakin, “Catenary curve,” pp. 1–26, 2019.

- [42] A. Hatibovic, “Parabola and Catenary Equations for Conductor Height Calculation,” vol. 60, no. 3, pp. 22–28, 2012.
- [43] S. J. Sugden, “Construction of transmission line catenary from survey data,” *Appl. Math. Model.*, vol. 18, no. 5, pp. 274–280, 1994, doi: 10.1016/0307-904X(94)90335-2.
- [44] “The catenary,” 1931.
- [45] O. C. Systems, “Catenary Design for Overhead Contact Systems,” no. 1, pp. 1082–1107, 1927.
- [46] *No Title.* .
- [47] F. V. B. De Nazaré and M. M. Werneck, “Temperature and current monitoring system for transmission lines using power-over-fiber technology,” *2010 IEEE Int. Instrum. Meas. Technol. Conf. I2MTC 2010 - Proc.*, pp. 779–784, 2010, doi: 10.1109/IMTC.2010.5488198.
- [48] E. Lindberg, “The Overhead Line Sag Dependence on Weather Parameters and Line Current,” no. December, p. 70, 2011.
- [49] I. Albizu and A. J. Mazon, “Factors that Affect the Sag-Tension Model of an Overhead Conductor.”
- [50] C. Baker and J. Baker, “Sag-Tension Calculation Program for Wood Pole Overhead Lines,” no. September 2013, 2016, doi: 10.1109/UPEC.2013.6715035.
- [51] J. Quintana, V. Garza, and C. Zamudio, “Sag-Tension Calculation Program for Power Substations (V),” pp. 968–972, 2016.

- [52] H. Dawood, *Interval mathematics as a potential weapon against uncertainty*, no. January 2014. 2014.
- [53] M. Carlo, “Monte Carlo Methods Outline What are Monte-Carlo methods ? Generation of random variables,” pp. 2010–2011, 2011.
- [54] M. Amelin, “Monte Carlo Simulation in Engineering,” 2013.
- [55] M. Firestone, P. Fenner-crisp, S. Chang, and M. Callahan, “Guiding Principles for Monte Carlo Analysis,” no. March, 1997.

Appendix

Appendix A. Metrological data of 10 cities

Appendix A. 1. Temperature annual data in degree centigrade

city	Year	Jan	Feb	Mar	Apr	May	Jun	Jul	Aug	Sep	Oct	Nov	Dec
Bahir Dar	2013	20.31	22.25	23.61	23.81	22.07	19.67	17.34	17.47	19.29	18.86	18.79	17.92
	2014	19.58	20.76	22.28	22.9	21.21	20.61	18.37	17.9	18.69	18.68	18.26	17.98
	2015	18.81	21.71	23.63	24.54	22.54	20.75	19.41	18.73	19.72	19.85	19.12	18.6
	2016	18.97	21.93	24.23	23.76	21.02	20.43	17.82	17.8	19.21	19.24	18.59	18.61
	2017	19.42	20.97	22.57	23.55	21.67	20.99	18.78	18.16	19.37	19.6	18.93	18.49
Dangila	2013	19.61	21.95	23.43	23.57	21.19	18.81	16.89	16.98	18.27	18	17.94	17.02
	2014	18.83	20.17	21.82	22.1	20.19	19.49	17.66	17.28	17.85	17.96	17.47	17.18
	2015	18.07	21.19	23.65	24.39	21.57	19.74	18.48	18.15	18.64	18.8	18.06	17.44
	2016	17.64	20.96	23.74	23.43	20	19.28	17.39	17.35	18.32	18.36	17.41	17.65
	2017	19.03	20.54	22.19	23.1	20.75	19.83	17.93	17.54	18.39	18.69	17.6	17.27
Enjibara	2013	20	22.35	23.72	23.72	20.91	18.73	16.88	17.02	18.28	18.1	17.99	17.15
	2014	19.14	20.56	22.14	21.89	20.14	19.42	17.57	17.36	17.93	18.12	17.59	17.25
	2015	18.23	21.36	23.74	24.59	21.2	19.56	18.43	18.1	18.66	18.87	18.12	17.65
	2016	18.02	21.22	23.8	23.33	19.78	19.12	17.41	17.38	18.38	18.55	17.21	17.47
	2017	18.68	20.82	22.58	22.98	20.6	19.86	17.83	17.56	18.45	18.82	17.61	17.07
Bura	2013	18.03	20.22	21.5	21.73	19.51	17.43	15.48	15.66	16.82	16.36	16.24	15.38
	2014	17.19	18.45	20.27	20.16	18.89	18.14	16.33	16.05	16.5	16.42	15.84	15.36
	2015	16.39	19.21	21.18	22.43	19.87	18.4	17.25	16.66	17.18	17.15	16.53	16.3
	2016	16.66	19.51	21.79	21.06	18.44	17.99	16.02	15.9	16.84	16.74	15.43	15.43
	2017	16.6	18.83	20.46	20.95	19.18	18.9	16.71	16.26	17.05	17.07	15.97	15.29
Finot Selam	2013	18.03	20.22	21.5	21.73	19.51	17.43	15.48	15.66	16.82	16.36	16.24	15.38
	2014	17.19	18.45	20.27	20.16	18.89	18.14	16.33	16.05	16.5	16.42	15.84	15.36
	2015	16.39	19.21	21.18	22.43	19.87	18.4	17.25	16.66	17.18	17.15	16.53	16.3
	2016	16.66	19.51	21.79	21.06	18.44	17.99	16.02	15.9	16.84	16.74	15.43	15.43
	2017	16.6	18.83	20.46	20.95	19.18	18.9	16.71	16.26	17.05	17.07	15.97	15.29

Worst-case Analysis of OHTL Parameters with Uncertainty using IA and MC approach

Debre Markos	2013	19.32	21.37	22.69	23.07	21.2	19.17	16.54	16.72	17.99	17.08	16.93	16.44
	2014	18.76	20.21	21.92	21.34	20.69	19.94	17.53	17.14	17.68	17.19	16.79	16.55
	2015	17.66	20.52	22	23.55	21.53	20.15	18.72	17.77	18.52	18.89	18.5	18.41
	2016	19.58	21.7	23.51	22.74	20.05	19.62	17.22	17.05	18.05	17.6	16.72	16.85
	2017	17.65	20.34	22.07	22.46	20.82	20.93	17.95	17.44	18.26	18.01	17.39	16.72
Dejen	2013	19.2	20.94	22.12	22.51	21.62	19.9	16.55	16.69	17.92	16.71	16.59	16.48
	2014	18.93	20.4	21.43	20.8	20.91	20.67	17.91	17.23	17.54	16.73	16.71	16.63
	2015	17.8	20.34	21.29	22.62	21.51	20.58	19.17	17.87	18.48	18.85	18.57	18.65
	2016	20.16	21.49	22.91	22.2	20.11	20.05	17.32	17.13	17.91	17.2	16.72	16.79
	2017	17.39	19.81	21.44	21.68	20.58	21.63	18.26	17.54	18.19	17.61	17.27	16.71
Gerbe Gurach	2013	19.31	21.02	22.27	22.04	21.15	19.28	16.31	16.53	17.72	16.63	16.46	16.43
	2014	19.22	20.48	21.64	20.93	21.17	20.62	17.66	17.16	17.43	16.81	16.78	16.76
	2015	17.83	20.28	21.49	22.79	21.4	20.25	18.82	17.71	18.38	19.02	18.88	18.87
	2016	20.42	21.61	22.92	22.18	20.02	19.75	17.22	17.01	17.67	17.11	16.62	16.73
	2017	17.21	19.95	21.2	21.65	20.34	21.19	17.85	17.39	17.95	17.57	17.04	16.35
Ficha	2013	17.46	18.76	20.35	20.29	20.07	18.72	15.55	15.9	16.72	15.36	15.08	14.95
	2014	17.67	18.87	19.48	18.93	19.44	19.81	17.14	16.58	16.37	15.41	15.41	15.33
	2015	16.15	18.26	19.44	20.54	20	19.35	18.2	17.09	17.44	17.23	16.86	16.93
	2016	18.58	19.35	20.81	20.25	18.73	18.67	16.54	16.22	16.61	15.68	15.03	14.74
	2017	15.11	18.13	19.32	19.5	18.89	20.34	17.29	16.73	16.83	16.18	15.33	14.55
Addis Ababa	2013	15.71	16.99	18.49	17.92	17.63	16.82	14.51	14.68	14.94	13.6	13.31	13.14
	2014	15.69	16.95	17.45	16.93	17.26	17.69	15.76	15.39	14.71	13.63	13.64	13.52
	2015	14.19	16.61	17.74	18.93	18.06	17.51	16.49	15.72	15.67	15.14	14.81	15
	2016	16.23	17.44	18.77	18.28	16.71	16.88	15.48	15.07	14.97	13.73	13.13	12.78
	2017	13.3	16.13	17.2	17.49	17.02	18.31	15.86	15.52	15.04	14.24	13.31	12.56

**Data source. National aeronautics and space administration (NASA) & Metrological Agency*

Appendix A. 2. Wind speed annual data in m/s

city	Year	Jan	Feb	Mar	Apr	May	Jun	Jul	Aug	Sep	Oct	Nov	Dec
Bahir	2013	3.51	4.17	4.09	3.9	4.01	3.55	3.73	3.54	2.96	3.19	3.49	3.22
	2014	3.57	4.23	3.57	3.96	3.44	3.91	3.57	3.12	3.21	3.29	3.42	3.28
Dar	2015	3.44	3.74	3.73	3.69	4.03	3.96	3.26	3.07	2.94	3.56	3.56	3.56

Worst-case Analysis of OHTL Parameters with Uncertainty using IA and MC approach

	2016	4.03	4.1	3.6	4.07	3.57	3.72	3.61	3.37	3.08	3.28	3.19	4.02
	2017	3.58	3.75	3.8	3.93	3.1	3.74	3.54	3.49	3.32	3.32	3.27	3.2
Dangila	2013	3.67	4.22	4.38	4.06	3.49	2.92	3.26	3.38	2.85	3	3.25	3.24
	2014	3.71	4.53	3.64	3.41	3.27	3.4	3.2	3.05	3.02	3.08	3.24	3.19
	2015	3.67	3.94	3.63	3.66	3.66	3.54	2.88	2.83	2.82	3.38	3.36	3.55
	2016	4.19	4.22	3.79	4.29	3.21	3.07	3.23	3.23	3.03	3.01	3.07	3.68
	2017	3.55	3.96	4.35	3.49	2.91	3.21	2.96	3.22	3.06	3.17	3.17	3.16
Enjibara	2013	3.48	4.01	4.29	4.01	3.34	2.8	3.13	3.2	2.54	2.68	2.97	3.01
	2014	3.42	4.38	3.61	3.07	3.13	3.11	3.07	2.86	2.69	2.85	3.15	3.1
	2015	3.53	3.6	3.31	3.57	3.29	3.25	2.72	2.68	2.57	3.4	3.39	3.61
	2016	4.17	4.17	3.6	4.21	2.95	2.96	3.1	3.1	2.79	2.88	3.2	3.68
	2017	3.72	3.77	4.27	3.34	2.77	2.96	2.84	3.11	2.73	3.06	3.18	3.13
Bura	2013	3.06	3.52	3.73	3.42	3.34	2.92	2.85	2.58	2.38	2.64	2.88	2.79
	2014	3.04	3.91	3.23	2.97	3.06	3.29	2.7	2.32	2.53	2.78	3.07	3.02
	2015	3.12	2.96	2.89	2.91	3.36	3.33	2.49	2.3	2.58	3.4	3.19	3.26
	2016	3.93	3.73	3.14	3.79	2.85	2.97	2.81	2.63	2.57	2.82	3.12	3.62
	2017	3.24	3.29	3.65	3.11	2.61	2.86	2.51	2.54	2.51	3.01	2.95	2.9
Finot Selam	2013	3.06	3.52	3.73	3.42	3.34	2.92	2.85	2.58	2.38	2.64	2.88	2.79
	2014	3.04	3.91	3.23	2.97	3.06	3.29	2.7	2.32	2.53	2.78	3.07	3.02
	2015	3.12	2.96	2.89	2.91	3.36	3.33	2.49	2.3	2.58	3.4	3.19	3.26
	2016	3.93	3.73	3.14	3.79	2.85	2.97	2.81	2.63	2.57	2.82	3.12	3.62
	2017	3.24	3.29	3.65	3.11	2.61	2.86	2.51	2.54	2.51	3.01	2.95	2.9
Debre Markos	2013	2.22	2.58	2.37	2.01	2.01	2.21	2.48	2.14	1.85	2.36	2.44	2.22
	2014	2.15	2.66	2.28	2.68	2.1	2.26	2.17	1.87	1.83	2.55	2.64	2.42
	2015	2.29	2.19	2.77	2.28	2.3	2.25	1.77	1.86	1.78	2.88	2.61	2.12
	2016	2.65	2.43	2.38	2.38	1.8	1.91	2.41	2.14	1.76	2.53	2.85	3.33
	2017	2.71	2.28	2.57	2.92	1.88	1.8	2.03	2.05	1.76	2.66	2.33	2.45
Dejen	2013	1.93	2.57	2.03	1.83	2	1.93	2.23	1.8	1.8	2.3	2.33	1.85
	2014	1.87	2.19	2.44	3.29	2.55	2.15	1.84	1.51	1.78	2.56	2.41	2.08

Worst-case Analysis of OHTL Parameters with Uncertainty using IA and MC approach

	2015	2.09	2.15	3.03	3.11	2.6	2.22	1.6	1.65	1.8	3.18	2.87	2.08
	2016	2.19	2.19	2.53	1.94	1.92	1.87	2.13	1.77	1.69	2.6	2.63	3.1
	2017	2.55	2.19	2.33	3.53	2.19	2.05	1.85	1.74	1.69	2.68	2.46	2.2
Gerbe	2013	2.22	2.86	2.23	1.9	1.74	1.78	2.23	1.84	1.74	2.49	2.6	2.1
Gurach	2014	1.86	2.27	2.59	3.27	2.39	2.16	1.87	1.64	1.79	2.67	2.64	2.2
	2015	2.3	2.37	3.25	3.18	2.5	2.19	1.54	1.65	1.8	3.12	2.89	2.12
	2016	2	2.3	2.67	1.98	1.91	1.91	2.14	1.84	1.83	2.74	2.83	3.33
	2017	2.9	2.31	2.3	3.63	2.16	2	1.91	1.83	1.76	2.85	2.63	2.51
Ficha	2013	3.09	3.88	2.86	2.65	2.66	1.91	2.47	1.98	2.34	3.19	3.42	2.79
	2014	2.48	2.74	3.64	4.26	3.48	2.71	2.06	1.68	2.39	3.56	3.54	2.96
	2015	3.15	3.41	4.24	4.19	3.43	2.64	1.89	1.85	2.58	4.25	3.97	3.2
	2016	2.56	3.22	3.53	2.43	2.76	2.6	2.26	2.17	2.36	3.59	3.59	4.16
	2017	3.78	3.07	3.21	4.54	2.97	2.91	2.16	1.99	2.36	3.69	3.57	3.18
Addis	2013	3.8	4.69	3.18	2.88	3.1	2.27	3.25	2.39	2.89	4.06	4.36	3.29
Ababa	2014	3.18	2.99	4.42	5.11	4.18	3.3	2.5	2.09	2.97	4.42	4.55	3.52
	2015	3.89	4.22	5.28	4.93	4.15	3.02	2.36	2.22	3.26	5.28	4.81	4.04
	2016	3.12	3.85	4.4	2.65	3.44	2.89	2.82	2.72	3	4.54	4.57	5.11
	2017	4.63	4.24	4.11	5.51	3.64	3.21	2.62	2.44	2.99	4.71	4.49	3.85

*Data source. National aeronautics and space administration (NASA) & Metrological Agency

Appendix B. Sag and tension data of case study area

Stringing Chart Report

Section #32 from structure #255 to structure #256
 Cable 'aster 851', Ruling span (m) 123.338
 Sagging data: Catenary (m) 1822.3 Condition C Temperature (deg C) 20
 Results below for condition 'Initial RS'
 Calculations done using actual span lengths and vertical projections

Span Length	Mid Span	Mid Span	Mid Span	Mid Span	Mid Span	Mid Span	Mid Span	Mid Span	Mid Span	Mid Span	Mid Span	Left Struct	Span Vertical
	Sag	Sag	Sag	Sag	Sag	Sag	Sag	Sag	Sag	Sag	Sag	Number	Projection
	5 C	10 C	15 C	20 C	25 C	30 C	35 C	40 C	45 C	50 C			(m)
	(m)	(m)	(m)	(m)	(m)	(m)	(m)	(m)	(m)	(m)	(m)		(m)
123.9	0.55	0.58	0.62	0.66	0.71	0.76	0.82	0.89	0.96	1.05	255		-6.13

Worst-case Analysis of OHTL Parameters with Uncertainty using IA and MC approach

CSDD NO. BBDA LOT 3A-TL-400-OL-C-DO-008-A RUNNING SAS TABLE FOR OPGW

Horiz Tension	Horiz Tension	Horiz Tension	Horiz Tension	Horiz Tension	Horiz Tension	Horiz Tension	Horiz Tension	Horiz Tension	Horiz Tension
5 C	10 C	15 C	20 C	25 C	30 C	35 C	40 C	45 C	50 C
(N)	(N)	(N)	(N)	(N)	(N)	(N)	(N)	(N)	(N)
14544	13821	13097	12391	11720	11049	10414	9814	9240	8701

*Data source. Ethiopian Electric Power Utility-Bahir Dar district. #32 section from Structure #255 to #256

Appendix C. Mat lab codes to generate results

Appendix C. 1. Mat lab codes for IA

```

1  WeightAA.m
2  Wb=1.5819;%lb/ft |Weight of the bare conductor
3  A=1.3185;%inch square area of the bare conductor
4  l=404.662;%ft span length
5  k=0;%Weight constant
6  Roa=0.0360;
7  Roa=0.0431;|
8  alpha=0.002383;
9  FW=WindPAA;
10 d=2*(sqrt(A/pi));
11 Wice=0;%lb since there is no ice accumulation in our conductors
12 Wwind=(d/12)*FW;%lb since ice thichnes is zero it can be ignored=(Pw(d+2*t)/12)
13 for i=1:12
14   Wtt(i,:)=sri(conaddi((multi(Wwind(i,:),Wwind(i,:))),(Wb^2)));
15 end
16 %%%Tension Calculator
17 at=19.3*10^-6;%Thermal Expansion Constant
18 E=11.5*10^6;%ELongation Constant
19 T=TempAA;%Measure temprature of the area in max and min retrieved from function called Temp
20 T0=20;%Initial Temprature
21 H0=2784.4945;%initial Tension%for check
22 c=0;%creep constant
23 for i=1:12
24   for j=1:2
25     k1(i,j)=(1+((Wtt(i,j)^2*l^2)/(24*H0^2)))*(1+at*(T(i,j)-T0))*(1/(E*A));
26     k2(i,j)=(1+((Wtt(i,j)^2*l^2)/(24*H0^2)))*(1+at*(T(i,j)-T0))*(1-(H0/(E*A))+c)-1;
27     k3(i,j)=0;
28     k4(i,j)=-(Wtt(i,j)^2*l^2)/24;
29     d=roots([k1(i,j) k2(i,j) k3(i,j) k4(i,j)]);
30     for ii=1:3
31       if(imag(d(ii))==0)
32         Ten(i,j)=real(d(ii));
33       end
34     end
35   end
36 for i=1:12
37   if(Ten(i,1)>Ten(i,2))
38     STen(i,:)=[Ten(i,2) Ten(i,1)];%swaping to make it min and max since tension decreases when tempratur

```


Worst-case Analysis of OHTL Parameters with Uncertainty using IA and MC approach

```

Editor - C:\Users\Moges Shiferaw\Desktop\Thesis results&cods\IA\10.Adiseabeba IA\WeightAA.m
WeightAA.m
46 dtt(i,:) = multi(divi(H00, Wtt(i,:)), conaddi(coshi(divi((1*Wtt(i,:), (2*H00))), -1));
47 end
48 %%%Length calculation
49 for i=1:12
50 Ltt(i,:) = conaddi((8*(multi(dtt(i,:), dtt(i,:)))/(3*1)), 1);
51 end
52 %%%DC and Ac resistance
53 for i=1:12
54 R(i,:) = Ro*(1+alpha*(68-T(i,:)));
55 RAC(i,:) = Roa*(1+alpha*(167-T(i,:)));
56 end
57 Rid(i,:) = (Ltt(i,:) .* R(i,:));
58 Ric(i,:) = (Ltt(i,:) .* RAC(i,:));
59 %%%generating graphs
60 figure(1); subplot(2,2,1)
61 plot(Wtt);
62 x=linspace(0.5,12.5);
63 xlabel('Months (Jan-Dec)');
64 ylabel('WR');
65 title(['Resultant weight']);
...
Command Window

```

Appendix C. 2. Mat lab codes for MC

```

Moges Shiferaw Desktop Thesis results&cods MC 1. Bahirdar MC
Editor - C:\Users\Moges Shiferaw\Desktop\Thesis results&cods\MC\1. Bahirdar MC\WeightBDRMC.m
WeightBDRMC.m
1 Wb=1.5819;%lb/ft |Weight of the bare conductor
2 A=1.3185;%inch square area of the bare conductor
3 k=0;%Weight constant
4 l=404.662;%ft span length
5 k=0;%Weight constant
6 Ro=0.0360;
7 Roa=0.0431;
8 alpha=0.002383;|
9 PW=WindPBDRMC;
10 d=2*(sqrt(A/pi));
11 Wice=0;%lb since there is no ice accumulation in our conductors
12 U=input('Enter the number of random Variables to be generated=');
13 PWU=zeros(12,U);%creating a space for the value
14 PWM=zeros(12,U);%creating a space for the value
15 WT=zeros(12,U);%creating a space for the value for squarooting the end result wind loading
16 MTenU=zeros(12,U);%creating a space for the value for TensionUppered
17 Sag=zeros(12,U);%creating a space for sag
18 MTEN=zeros(12,U);%creating a space for the value for tension final
19 Len=zeros(12,U);%creating a space for the value forlength
20
Command Window

```

```

Moges Shiferaw Desktop Thesis results&cods MC 1. Bahirdar MC
Editor - C:\Users\Moges Shiferaw\Desktop\Thesis results&cods\MC\1. Bahirdar MC\WeightBDRMC.m
WeightBDRMC.m
19 Len=zeros(12,U);%creating a space for the value forlength
20
21 for i=1:12
22 PWU(i,:) = (PW(i,2) - PW(i,1)) .* rand(1,U);
23 PWM(i,:) = bsxfun(@plus, PWU(i,:), PW(i,1));% Monte carlo generated variables with the wind pres
24 end
25 Wwind = (d/12) * PWM;%lb since ice thichnes is zero it can be ignored=(Pw(d+2*t)/12)
26 WTS=Wwind .* Wwind;
27 for i=1:12
28 WT(i,:) = sqrt(bsxfun(@plus, WTS(i,:), Wb^2));%Monte Carlo Resultant Weight
29 end
30 % Final Wight in interval
31 for i=1:12% Boundery based weight
32 mnmx(i,:) = [min(WT(i,:)) max(WT(i,:))]; %the monte carlo total weight in interval
33 end
34 Wtm = mnmx; %equating the weight to the variable Wtm(Total Wight monte carlo)
35 %%%Tension Calculator
36 at=19.3*10^-6;%Thermal Expansion Constant
37 E=11.5*10^6;%ELongation Constant
38 T=TempBDRMC%Measure temprature of the area in max and min retrieved from function called Temp
...
Command Window

```

Worst-case Analysis of OHTL Parameters with Uncertainty using IA and MC approach

```

Moges Shiferaw > Desktop > Thesis results&cods > MC > 1. Bahirdar MC
Editor - C:\Users\Moges Shiferaw\Desktop\Thesis results&cods\MC\1. Bahirdar MC\WeightBDRMC.m
WeightBDRMC.m
40 - H0=2784.4945;%initial Tension
41 - c=0;%creep constant
42 - for i=1:12
43 -     for j=1:2
44 -         k1(i,j)=(1+((Wtm(i,j)^2*1^2)/(24*H0^2)))*(1+at*(T(i,j)-T0))*(1/(E*A));
45 -         k2(i,j)=(1+((Wtm(i,j)^2*1^2)/(24*H0^2)))*(1+at*(T(i,j)-T0))*(1-(H0/(E*A))+c)-1;
46 -         k3(i,j)=0;
47 -         k4(i,j)=- (Wtm(i,j)^2*1^2)/24;
48 -         d=roots([k1(i,j) k2(i,j) k3(i,j) k4(i,j)]);
49 -
50 -
51 -     for ii=1:3
52 -         if(imag(d(ii))==0)
53 -             Ten(i,j)=real(d(ii));
54 -         end
55 -     end
56 - end
57 - end
58 - %%Tension Final Interval
59 - for i=1:12

```

```

Moges Shiferaw > Desktop > Thesis results&cods > MC > 1. Bahirdar MC
Editor - C:\Users\Moges Shiferaw\Desktop\Thesis results&cods\MC\1. Bahirdar MC\WeightBDRMC.m
WeightBDRMC.m
58 - %%Tension Final Interval
59 - for i=1:12
60 -     if(Ten(i,1)>Ten(i,2))
61 -         MTen(i,:)=[Ten(i,2) Ten(i,1)];%swaping to make it min and max since
62 -     else
63 -         MTen(i,:)=[Ten(i,1) Ten(i,2)];
64 -     end
65 - end
66 - %%Tension in Monte Carlo
67 - for i=1:12
68 -     MTenU(i,:)=(MTen(i,2)-MTen(i,1)).*rand(1,U);
69 -     MTEN(i,:)=bsxfun(@plus,MTenU(i,:), MTen(i,1));% Monte carlo
70 - end
71 - %%sag Calculation
72 - for i=1:12
73 -     for j=1:U
74 -         Sag(i,j)=(H0/WT(i,j))*((cosh((WT(i,j)*1)/(2*H0)))-1);
75 -     end
76 - end
77 -

```

```

Moges Shiferaw > Desktop > Thesis results&cods > MC > 1. Bahirdar MC
Editor - C:\Users\Moges Shiferaw\Desktop\Thesis results&cods\MC\1. Bahirdar MC\WeightBDRMC.m
WeightBDRMC.m
79 - for i=1:12% Boundary based weight
80 -     minmxS(i,:)=[min(Sag(i,:)) max(Sag(i,:))]; %the monte carlo sag in interval
81 - end
82 - %%
83 - %% %%%Length calculation
84 - %%
85 - for i=1:12
86 -     for j=1:U
87 -         Len(i,j)=(2*H0/WT(i,j))*(sinh((WT(i,j)*1)/(2*H0)));
88 -     end
89 - end
90 - %%Length Final Interval
91 - for i=1:12%
92 -     minmxL(i,:)=[min(Len(i,:)) max(Len(i,:))]; %the monte carlo length in interval
93 - end
94 - %%DC and Ac resistance
95 - for i=1:12
96 -     RM(i,:)=Ro*(1+alpha*(68-T(i,:)));
97 -     RMAC(i,:)=Roac*(1+alpha*(167-T(i,:)));
98 - end

```

Appendix D. Contents of the table used for result demonstration

Appendix D. 1. Table I

Table I consists of many tables for 10 cites that is Table 1, Table 4, Table 7, Table 10, Table 13, Table 16, Table 19, Table 22, Table 25, and Table 28.

Appendix D. 2. Table II

Table II consists of many tables for 10 cites that is Table 2, Table 5, Table 8, Table 11, Table 14, Table 17, Table 20, Table 23, Table 26, and Table 29.

Appendix D. 3. Table III

Table III consists of many tables for 10 cites that is Table 3, Table 6, Table 9, Table 12, Table 15, Table 18, Table 21, Table 24, Table 27, and Table 30.